NOTICE

The quality of this microform is heavily dependent upon the quality of the original thesis submitted for microfilming. Every effort has been made to ensure the highest quality of reproduction possible.

If pages are missing, contact the university which granted the degree.

Some pages may have indistinct print especially if the original pages were typed with a poor typewriter ribbon or if the university sent us an inferior photocopy.

Reproduction in full or in part of this microform is governed by the Canadian Copyright Act, R.S.C. 1970, c. C-30, and subsequent amendments.

AVIS

La qualité de cette microforme dépend grandement de la qualité de la thèse soumise au microfilmage. Nous avons tout fait pour assurer une qualité supérieure de reproduction.

S'il manque des pages, veuillez communiquer avec l'université qui a conféré le grade.

La qualité d'impression de certaines pages peut laisser à désirer, surtout si les pages originales ont été dactylographiées à l'aide d'un ruban usé ou si l'université nous a fait parvenir une photocopie de qualité inférieure.

La reproduction, même partielle, de cette microforme est soumise à la Loi canadienne sur le droit d'auteur, SRC 1970, c. C-30, et ses amendements subséquents.

Canada

Nitric Oxide Binding to Cytochrome c and Its Peroxidase

Paul Ala

A Thesis

in

The Department

of

Chemistry

Presented in Partial Fulfillment of the Requirements
for the Degree of Master of Science at
Concordia University
Montreal, Quebec, Canada

September 1989

Canada

ABSTRACT

Nitric Oxide binding to Cytochromes c and Its Peroxidase

Paul Ala

The equilibrium dissociation constants (K_D) for the formation of the nitric oxide adducts of ferricytochrome c peroxidase, CCP(III)-NO, and ferricytochrome c, cyt c(III)-NO, have been determined in 100 mM sodium phosphate buffer, at pH 7.0, and 23 °C. Equilibrium measurements for the binding of NO by CCP(III) and by cyt c(III) yielded K_D values of 44 ± 5 and 36 ± 3 μM, respectively. Moreover, the ratio of the kinetic rate constants (k_{off}/k_{on}) for NO binding to cyt c(III) is 65 ± 9 μM. The similarity between the kinetic and equilibrium binding parameters is consistent with a simple mechanism of ligand binding to monomeric hemoprotein [1].

The estimated rate of intracomplex electron transfer from CCP(II)-NO to cyt c(III) in the CCP/cyt c complex is ≥ 40 times slower than that from CCP(II) to cyt c(III). The decrease in the redox reactivity of CCP(II)-NO may be due in part to the repositioning of CCP residues on NO binding which are located along the proposed electron transfer pathway between the hemes of CCP and cyt c. Since the reduction potential for the Fe(III)/(II) couple of CCP increases by 250-300 mV on binding NO, the decrease in $\Delta E°$, may also contribute to the drop in the rate of electron transfer.

The association rate constants for NO binding to horse and yeast cyts c(III), in the presence and absence of CCP(III), have been determined in 10 mM sodium phosphate, at pH 7.0, and 23 °C. The bimolecular rate constants for the binding of NO to free and complexed horse and yeast cyts c(III) are 417 ± 60 and 305 ± 43 M^{-1} s^{-1}, and 365 ± 51 and 96 ± 13 M^{-1} s^{-1}, respectively. Therefore, complex formation reduces the rate of NO binding to the hemes of horse and yeast cyts c by 27-45% and 74%, respectively. These results suggest that CCP reduces the accessibility to the heme iron of cyt c, and/or binding of the negatively-charged peroxidase stabilizes the closed heme crevice structure of cyt c.

ACKNOWLEDGEMENTS

TABLE OF CONTENTS

CHAPTER 2

Effects of Nitric Oxide Coordination on The Redox Reactivity of Cytochrome c Peroxidase 48

CHAPTER 3

ABBREVIATIONS

NO	=	nitric oxide
CCP(III)	=	ferricytochrome c peroxidase
CCP(II)	=	ferrocytochrome c peroxidase
CCP-NO	=	nitrosylcytochrome c peroxidase
cyt c(III)	=	ferricytochrome c
cyt c(II)	=	ferrocytochrome c
cyt(s) c-NO	=	nitrosylcytochrome(s) c
CCP/cyt c	=	is the noncovalent complex formed between the proteins
Mb	=	myoglobin
k_{on}	=	association rate constant
k_{off}	=	dissociation rate constant
K_D	=	equilibrium dissociation constant

LIST OF FIGURES

LIST OF TABLES

INTRODUCTION

The elucidation of the physical and chemical nature of the heme environment provided by the protein is of importance in our understanding of the diversity of reactivity and functions of hemoproteins. Ligand binding studies are one of the most important tools for probing the active sites of hemoproteins. Valuable information about structure has been obtained by observing the effects of binding ligands such as CN⁻, HF, and NO, to various hemes.

Nitric oxide is a neutral small molecule and a powerful complexing agent. It forms stable adducts with both oxidation states of CCP [2] and cyt c(III) [3] at neutral pH. In the case of CCP, the hemes of both oxidation states are converted to low-spin states [2]. In cyt c(III), and not cyt c(II), NO replaces Met-80 as the sixth ligand [4].

. Binding of NO to CCP is an obvious choice for these studies since the crystal structures of both CCP(III) [5] and CCP(III)-NO [6] are known to high resolution. Also, the crystal structure of cyt c(III) [7] is known, and computer graphics modelling of the CCP/cyt c complex has been carried out by optimizing hydrogen bonding interactions between complementary charged groups [8]. In this work, NO is used as a kinetic probe to investigate the following topics:

Chapter 1: The ligand binding properties of CCP(III) and cyt c(III)

Chapter 2: The effect of ligand binding on the redox reactivity of CCP(II)

Chapter 3: The accessibility of the hemes of horse and yeast cyts c(III) in complexes with CCP(III)

CHAPTER 1

THE BINDING OF NITRIC OXIDE

BY

HEMOPROTEINS

1.1 INTRODUCTION

An equilibrium constant (K) defines the position of the equilibrium of a reaction. In a reversible system at equilibrium, the on and off rates are the same:

$$P + X \underset{k_{off}}{\overset{k_{on}}{\rightleftharpoons}} P\text{-}X \qquad (1.1)$$

Therefore, K can be defined as the ratio of the on and off rate constants, or as the ratio of the products and reactants:

$$K = \frac{k_{on}}{k_{off}} = \frac{[PX]_{eq}}{[P]_{eq}[X]_{eq}} \qquad (1.2)$$

Although equilibrium binding constants cannot provide individual rate constants, knowledge of these constants is necessary to predict the stability of intermediates and products in multistep reactions. This will become obvious, in the following chapters, when the results of studies on (1) electron transfer from CCP(II)-NO to cyt c(III), and (2) the accessibility of the heme of cyt c are presented.

A large number of equilibrium constants have been determined for heme protein adducts in an attempt to understand the physical environment and electronic nature of different hemes. The most commonly used ligands are carbon monoxide, oxygen and nitric oxide, and equilibrium dissociation constants of these heme

protein adducts are given in Table 1.I

It is interesting to note that K_D values for a given ligand vary a lot between different heme proteins as well as between different sources of the same protein. For example, elephant myoglobin-NO is approximately 130 times more stable than sperm whale myoglobin-NO even though the off-rate for elephant myoglobin-NO is $\approx$ 3 times faster than that of sperm whale myoglobin. This difference in K_D is due to the fact that elephant myoglobin reacts with NO 415 times faster than sperm whale myoglobin [9]. Differences in K_D are usually associated with variations in protein matrices and ligand binding sites which determine the magnitude of the on and off rates. Consequently, important information can be obtained from the comparison of equilibrium constants.

Equilibrium constants can be determined directly by titration or indirectly from kinetic measurements. In the former method, K_D is determined by measuring the concentrations of all species involved in the equilibrium following successive additions of ligand to protein. In the kinetic method, the on and off rate constants are determined and their ratio provides K (Eq 1.2). Here, we report the equilibrium constants for the binding of NO by CCP(III) and cyt c(III). The K_D for the binding of NO by CCP(III) was measured using equilibrium measurements, and by cyt c(III) via both equilibrium and kinetic measurements.

Table 1.I. Equilibrium Dissociation Constants (K_D) for Heme Protein

Adducts

Heme Protein	K_D (μM)		
	CO	$O_2{}^a$	NO^b
Myoglobin (sperm whale)	.03[a]	.67	264
Myoglobin (elephant)	---	---	2
Hemoglobin (carp)	.4[a]	40	929
Hemoglobin (human)	.056[c]	.56	---
CCP (yeast)	4.6[a]	---	---

[a] Ferroheme adducts; Isolated α chains of human

hemoglobin; Carp hemoglobin fast component at

pH 6.0; [10]

[b] Ferriheme adducts [9]

[c] Ferroheme adduct [11]

1.2 EXPERIMENTAL

MATERIALS-

Yeast CCP was isolated by the published procedure [12], and type VI horse heart cyt c was obtained from Sigma. The concentrations of CCP(III), CCP(III)-NO, cyt c(III), and cyt c(III)-NO were determined from their optical absorbance spectra using extinction coefficients of 98 and 50 mM^{-1} cm^{-1} at 408 and 424 nm [13]; 123 mM^{-1} cm^{-1} at 424 nm (this work); 106.1 and 70 mM^{-1} cm^{-1} at 410 and 418 nm [14]; and 122 mM^{-1} cm^{-1} at 418 nm [3], respectively. Nitric oxide (CP grade) was obtained from Union Carbide and was passed through KOH pellets before use to remove any higher oxides of nitrogen.

METHODS-

All equilibrium measurements were carried out with CCP and cyt c concentrations between 2 and 5 μM in 100 mM sodium phosphate, at pH 7.0, and 23 °C. Spectrophotometric titrations were carried out as follows: a known amount of either protein was dissolved in a sealed 1-cm cuvette containing enough deoxygenated buffer (or argon saturated buffer) so that only ≤ 0.3 mL (a small bubble) of argon gas remained in the cuvette. NO-saturated buffer was prepared by bubbling NO gas into 3 mL of deoxygenated buffer for 20 min. Aliquots of ≈ 20 μL of NO-saturated buffer (≈ 2 mM as calculated from the published Henry's Law constant [15]) were added to the cuvette using a gas-tight syringe. The formation of CCP(III)-NO and cyt c(III)-NO was monitored at 424 and 418 nm, respectively,

using an HP 8451A spectrophotometer. At the monitoring wavelength, absorbance changes of 0.17 and 0.3 were expected for 3.2 μM cyt c and 4.4 μM CCP as calculated from $\Delta\varepsilon$ (P-NO - P) of 52 mM^{-1} cm^{-1} and 73 mM^{-1} cm^{-1} the extinction coefficients given above. The data were analyzed as described in the next section.

Kinetic measurements were carried out with cyt c concentrations ranging from 3 to 5 μM in 10 mM sodium phosphate buffer, pH 7.0, 23 °C. Kinetic determinations of K_D were carried out as follows: lyopholyzed cyt c was dissolved in 50 mL of deoxygenated buffer in a 100 mL volumetric flask and degassed with argon for 30 min. NO-saturated buffer was prepared by bubbling NO into 50 mL of deoxygenated buffer in a 100 mL volumetric flask for $\approx$ 50 min. Both flasks were then attached to the stopped-flow unit. On-rates for the binding of NO by cyt c(III) were measured under pseudo first-order conditions at NO concentrations of 95 to 666 μM. This range of NO concentrations was obtained by simply changing the size (0.25, 0.5, 1.0 and 2.5 mL) of the syringe used to inject the NO-saturated buffer. All the reactions were monitored at 418 nm following rapid mixing in the 2-mm cuvette of a modified HI-TECH SFA-11 Fast Kinetics Accessory stopped-flow unit using the fast response time (0.1 s) of the HP Model 8451A spectrophotometer.

The SFA-11 was modified to minimize gas diffusion across the wall of the teflon tubing which connects the substrate reservoirs to the cuvette, by surrounding the teflon with zerohal heat shrinkable tubing obtained from Raychem Canada Ltd. The addition of heat shrinkable tubing increased the thickness of the wall of the connecting tubing by 3-4 fold. In addition, the kinetic experiments were performed in a glovebag to minimize NO oxidation by O_2.

1.3 DATA ANALYSES

1.31 EQUILIBRIUM DATA- The equilibrium contants were determined form Scatchard plots [16]. The equilibrium expression for the binding of protein [P] to [NO] is given by Eq 1.3:

$$[P] + [NO] \xrightleftharpoons[k_{off}]{k_{on}} [P-NO] \tag{1.3}$$
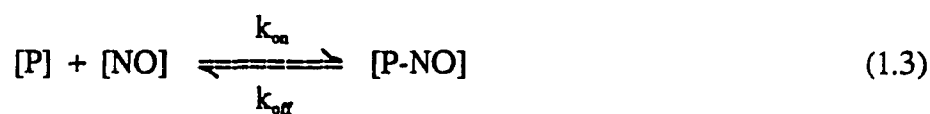
where $K = k_{on}/k_{off} = [P-NO]/[P][NO]$. The total concentration of protein $[P_o]$ is equal to the sum of free [P] and NO-bound protein [P-NO], i.e.,

$$[P_o] = [P] + [P-NO] \tag{1.4}$$

therefore,

$$[P] = [P_o] - [P-NO] \tag{1.5}$$

By substituting the expression for [P] from Eq 1.5 into Eq 1.3, the equilibrium expression can now be expressed as follows:

$$[P-NO]/[NO] = -K[P-NO] + K[P_o] \tag{1.6}$$

The concentration of [P-NO] is calculated from the expression $\Delta A/\Delta\varepsilon$, where ΔA is the observed absorbance minus the initial absorbance for each point in the titration, and $\Delta\varepsilon$ is the difference in extinction coefficients between [P-NO] and [P] at a fixed wavelength. The concentration of free NO can be set equal to the total concentration, $[NO]_T$, since $[NO]_T \gg [P_o]$ under conditions where the formation of [P-NO] is observed. Therefore, Eq 1.6 can be written as follows:

$$\Delta A/[NO] = K\Delta\varepsilon[P_o] - K\Delta A \tag{1.7}$$

A plot of $\Delta A/[NO]$ versus ΔA is called a Scatchard Plot, where the slope is equal to -K.

1.32 KINETIC DATA- The observed rate constants (k_{obs}), which are pseudo first-order with respect to the protein concentration, for the binding of NO by cyt c(III) were obtained by computer analyses using the Simplex nonlinear regression method [17]. The expression for the observed rate constant is given by Eq 1.8 [18]:

$$k_{obs} = k_{on} [NO]_T + k_{off} \tag{1.8}$$

A plot of k_{obs} vs. [NO] yields the values of k_{off} and k_{on} from the intercept and slope, respectively, for the reaction:

$$\text{cyt c(III)} + \text{NO} \underset{}{\overset{K}{\rightleftharpoons}} \text{cyt c(III)-NO} \tag{1.9}$$
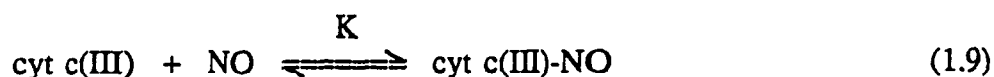
where, $K = k_{on}/k_{off} = [\text{cyt c-NO}]/[\text{cyt c}] [NO]$

1.4 RESULTS

1.41 Spectrophotometric Titration of CCP(III) with NO.

The absorbance spectra of CCP and its NO adduct are shown in Figure 1.1. Upon binding NO, the Soret maximum of CCP red shifts by 16 nm to 424 nm. In contrast, Yonetani et al. [2] have previously reported that CCP(III)-NO has a Soret maximum at 419 nm. The reason for this 5-nm discrepancy of the Soret maximum is not yet known. Figure 1.2 shows the difference spectrum between the NO adduct and CCP, and a typical spectrophotometric titration at 418 nm of CCP with NO is presented in Figure 1.3. An overlay of the spectra during the titration is given in Figure 1.4, and the appearance of isosbestic points indicates that there was no loss of protein during the course of an experiment and that no intermediates were formed.

Scatchard plots for CCP(III)-NO formation at various concentrations of CCP are presented in Figure 1.5. Nearly parallel lines indicates good reproducibility, and the K_D values from the slopes are given in Table 1.II (for raw data see Tables I-VII in Appendix A). The average K_D is 44 and the standard deviation is $\pm$ 5 μM.
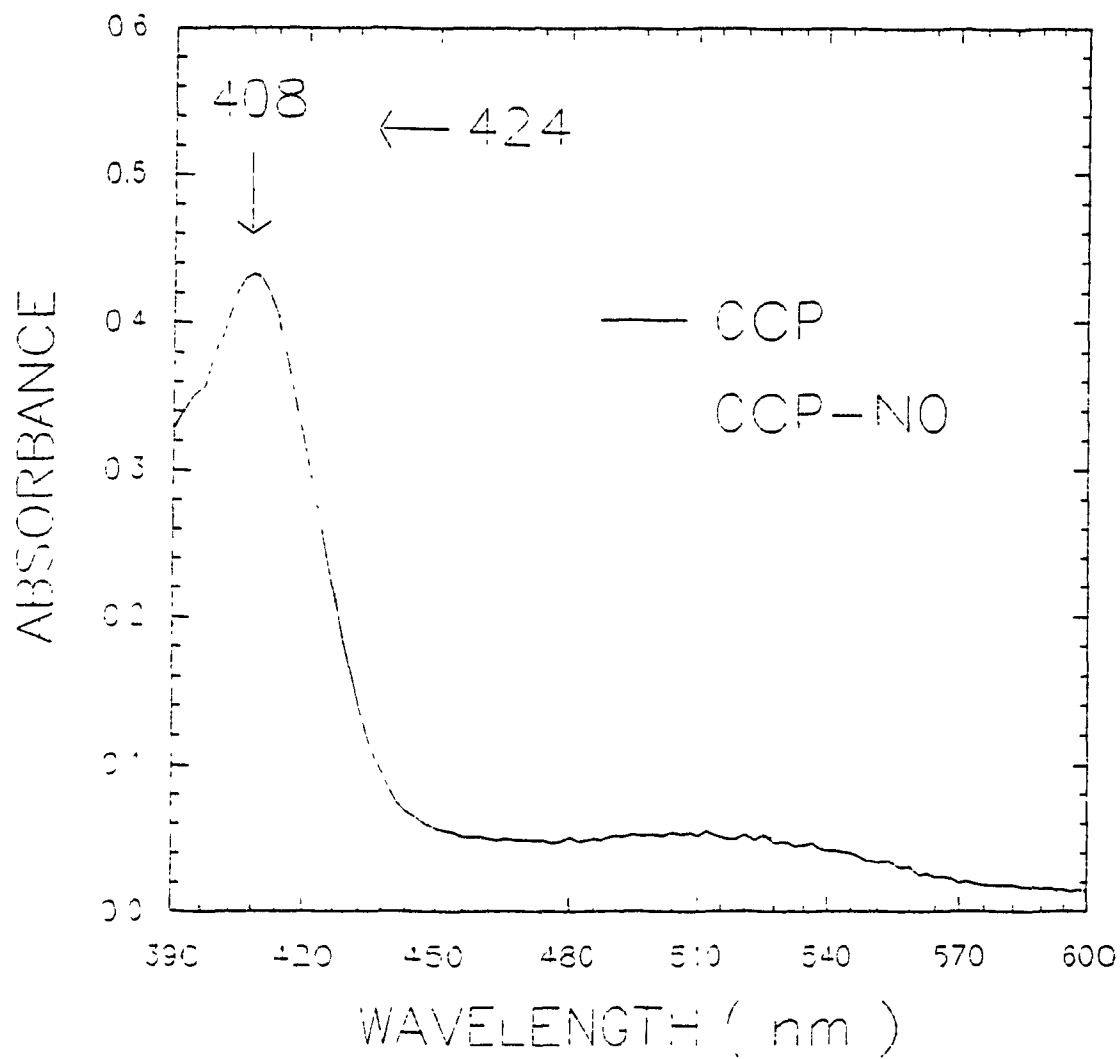
Figure 1.1. Absorption spectra of 4.4 μM CCP(III) (solid line) and its NO

adduct (dotted line) in 100 mM sodium phosphate, pH 7.0,

23 °C, 1-cm pathlength. [NO] = 100 μM
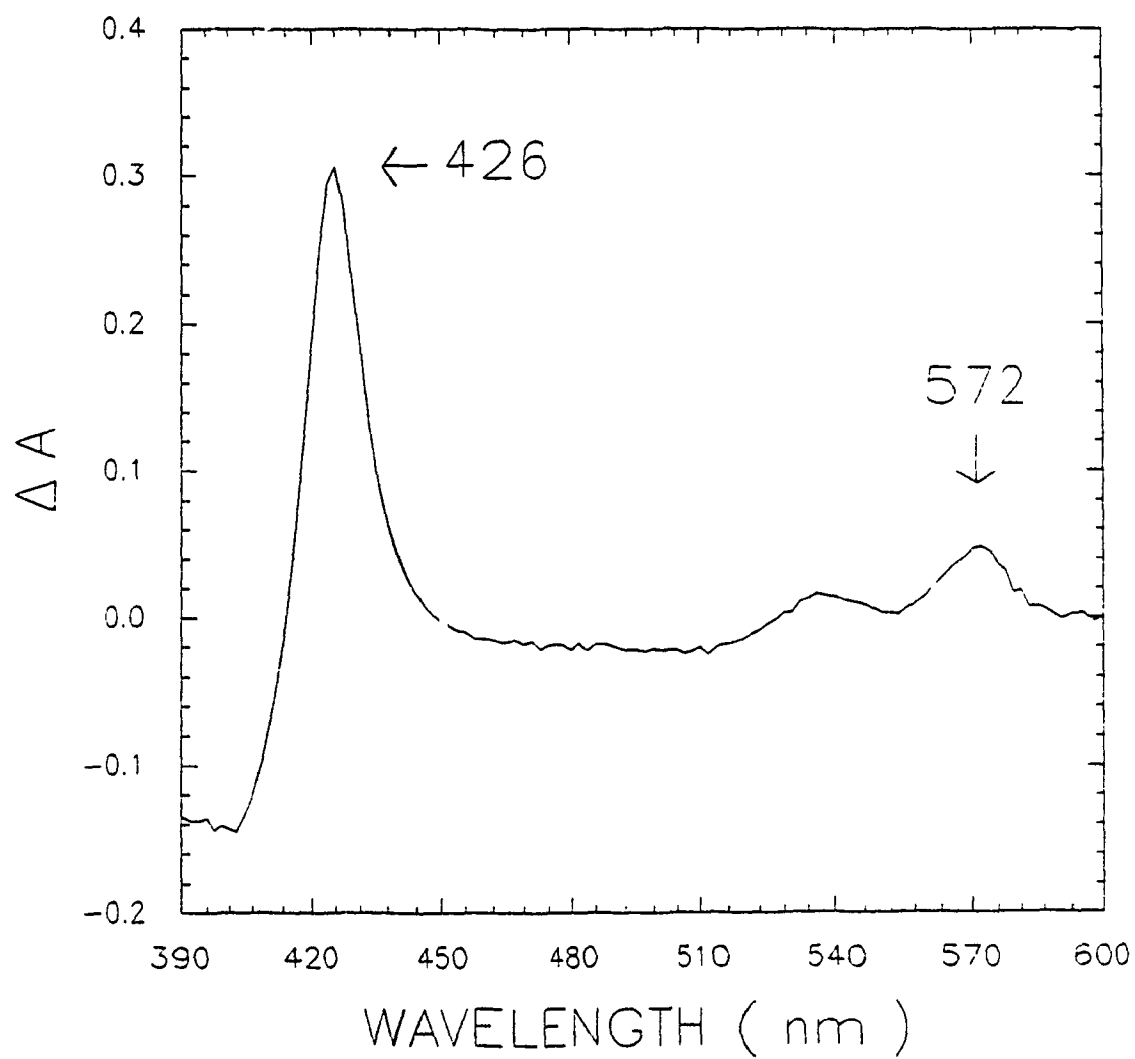
Figure 1.2   Difference spectrum between CCP(III)-NO and CCP(III).

Conditions as per Figure 1.1.
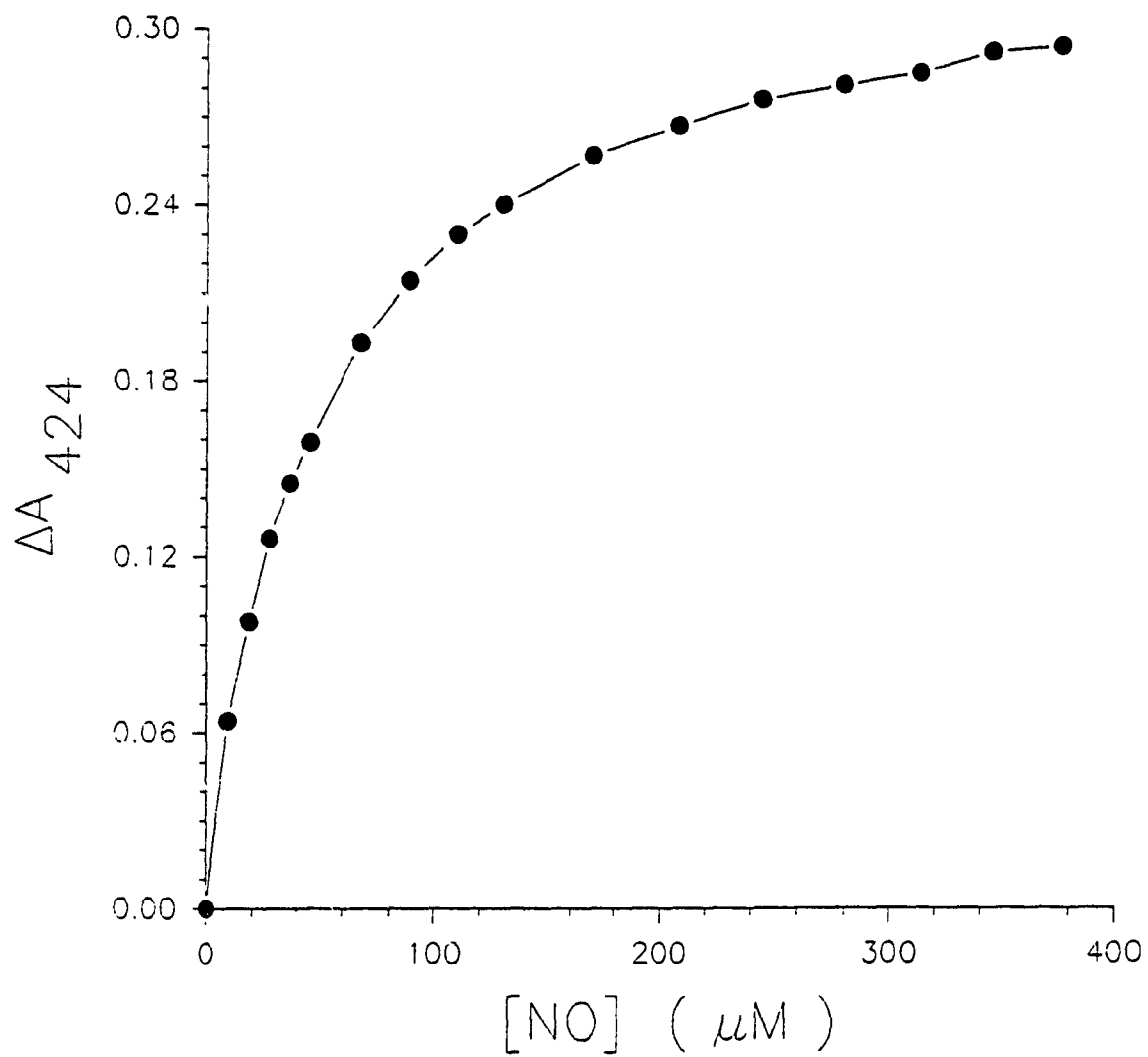
Figure 1.?   Spectrophotometric titration of 4.4 µM CCP(III)

at 424 nm with NO in 100 mM sodium phosphate,pH 7.0, 23 °C.
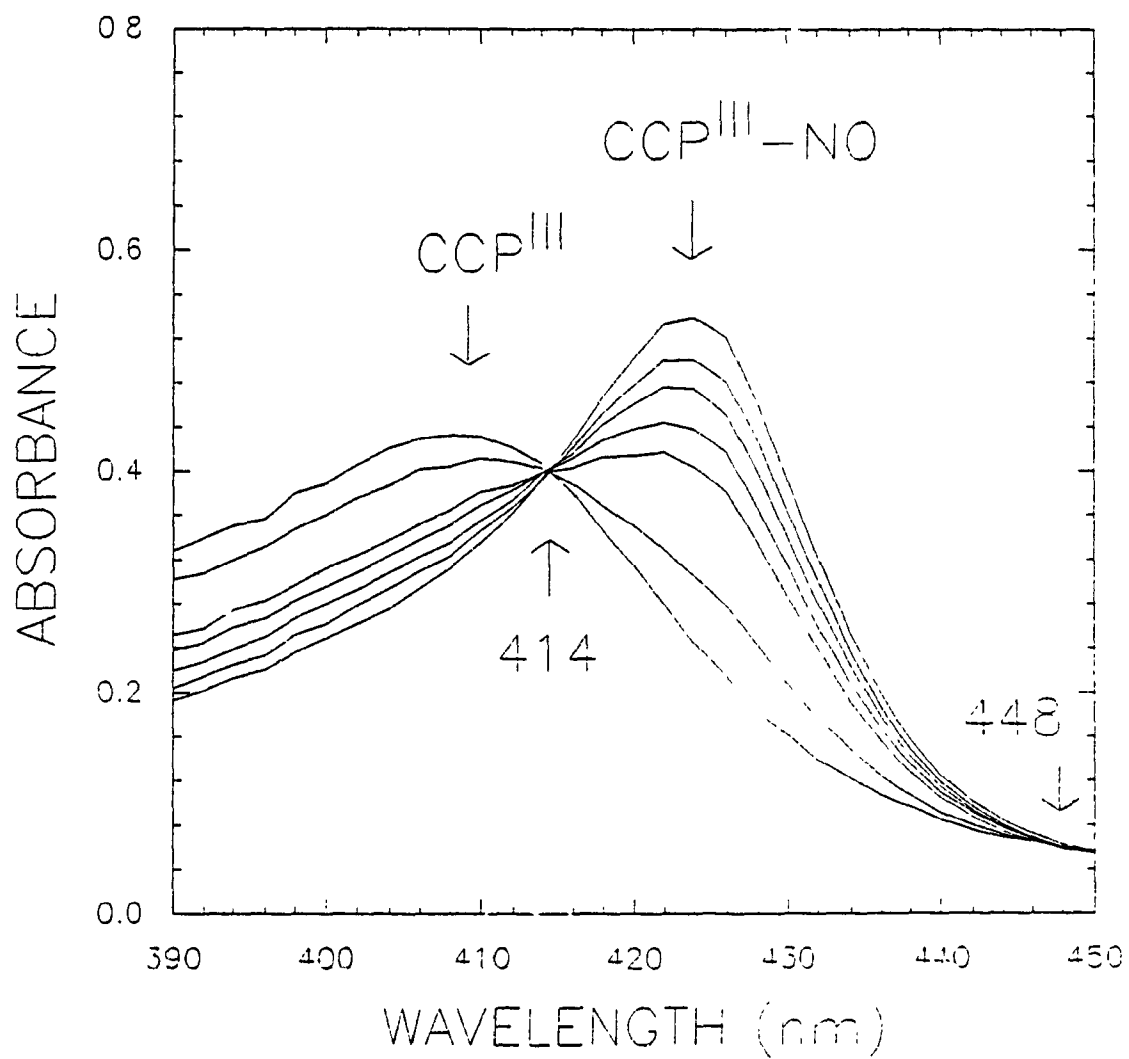
Figure 1.4. Overlay of spectra showing the conversion of free CCP(III) to CCP(III)-NO during the titration of CCP with NO. Conditions as per Figure 1.3. Note the isosbestic points at 414 and 448 nm.
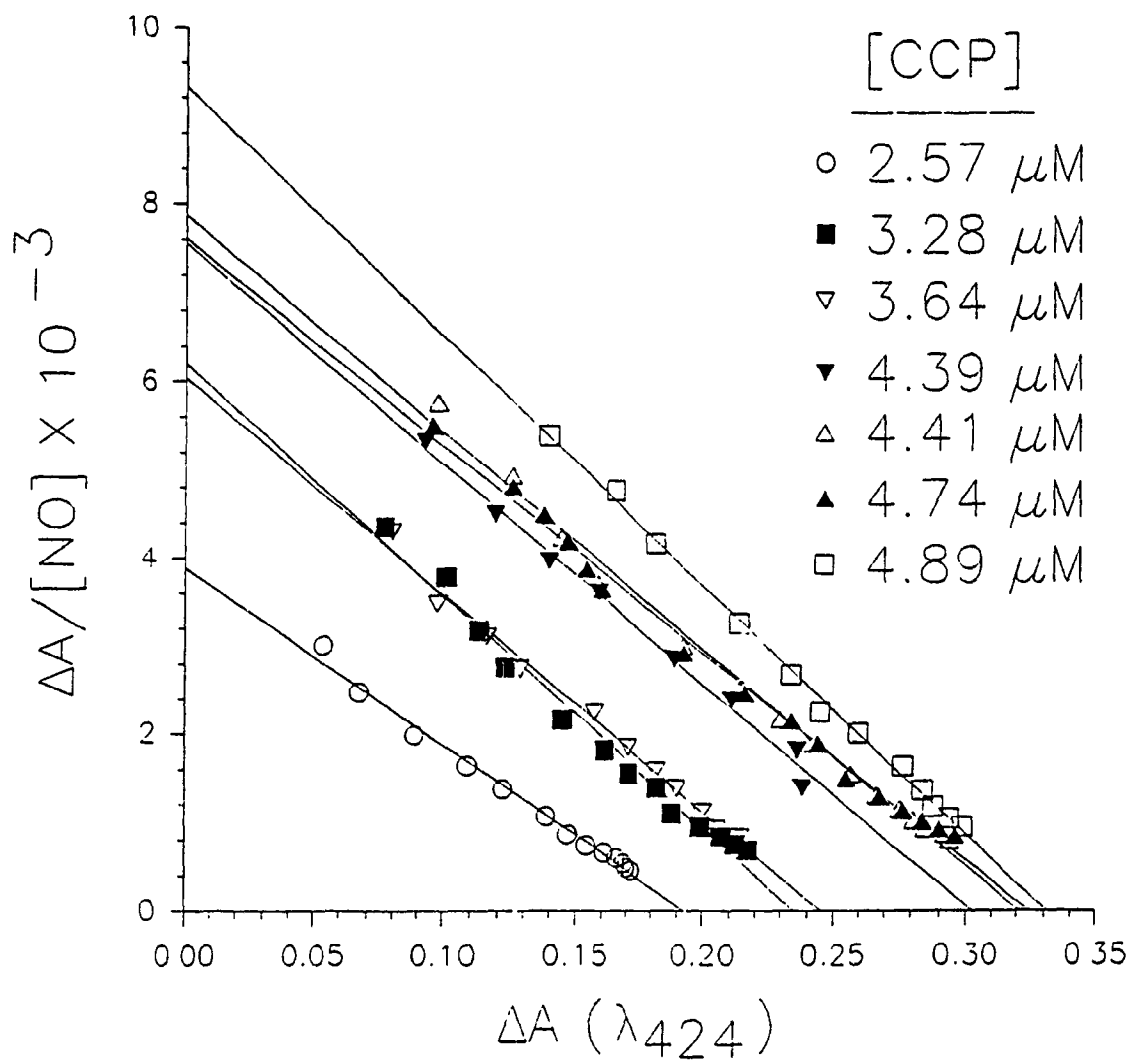
Figure 1.5. Scatchard plots for CCP(III)-NO formation at various concentrations of CCP. Conditions as per Figure 1.3. Data from Appendix A, Tables I-VII.

Table 1.II. Equilibrium Dissociation Constants for The Binding of NO by CCP(III) in 10 mM Sodium Phosphate Buffer, pH 7.0, 23 °C

[CCP] (μM)	K_D (μM)
2.57	52.1
3.28	40.7
3.64	43.6
4.39	44.2
4.41	44.5
4.74	45.2
4.89	35.1

1.42 Spectrophotometric Titration of Cyt c(III) with NO.

The absorption spectra of cyt c(III) and its nitrosyl adduct are shown in Figure 1.6. Upon binding NO, the Soret maximum of cyt c(III) red shifts by about 10 nm to 418 nm. The magnitude of this red shift is consistant with previously published data since Butt and Keilin [3] have also reported a shift in the Soret maximum of 9 nm to 417 nm upon binding NO. Figure 1.7 shows the difference spectrum between cyt c(III)-NO and free cyt c, and a typical spectrophotometric titration of cyt c(III) with NO at 418 nm is presented in Figure 1.8. An overlay of the spectra during the titration is presented in Figure 1.9, and the appearance of isosbestic points again indicates that there was no loss of protein during the course of an experiment and that no intermediates were formed.

Scatchard plots for cyt c(III)-NO formation at various concentrations of cyt c are presented in Figure 1.10. Once again, the existence of nearly parallel lines indicates good reproducibility, and the K_D values from the slopes are given in Table 1.III (for raw data see Tables I-III in Appendix B). The average K_D is 36 ± 3 μM.
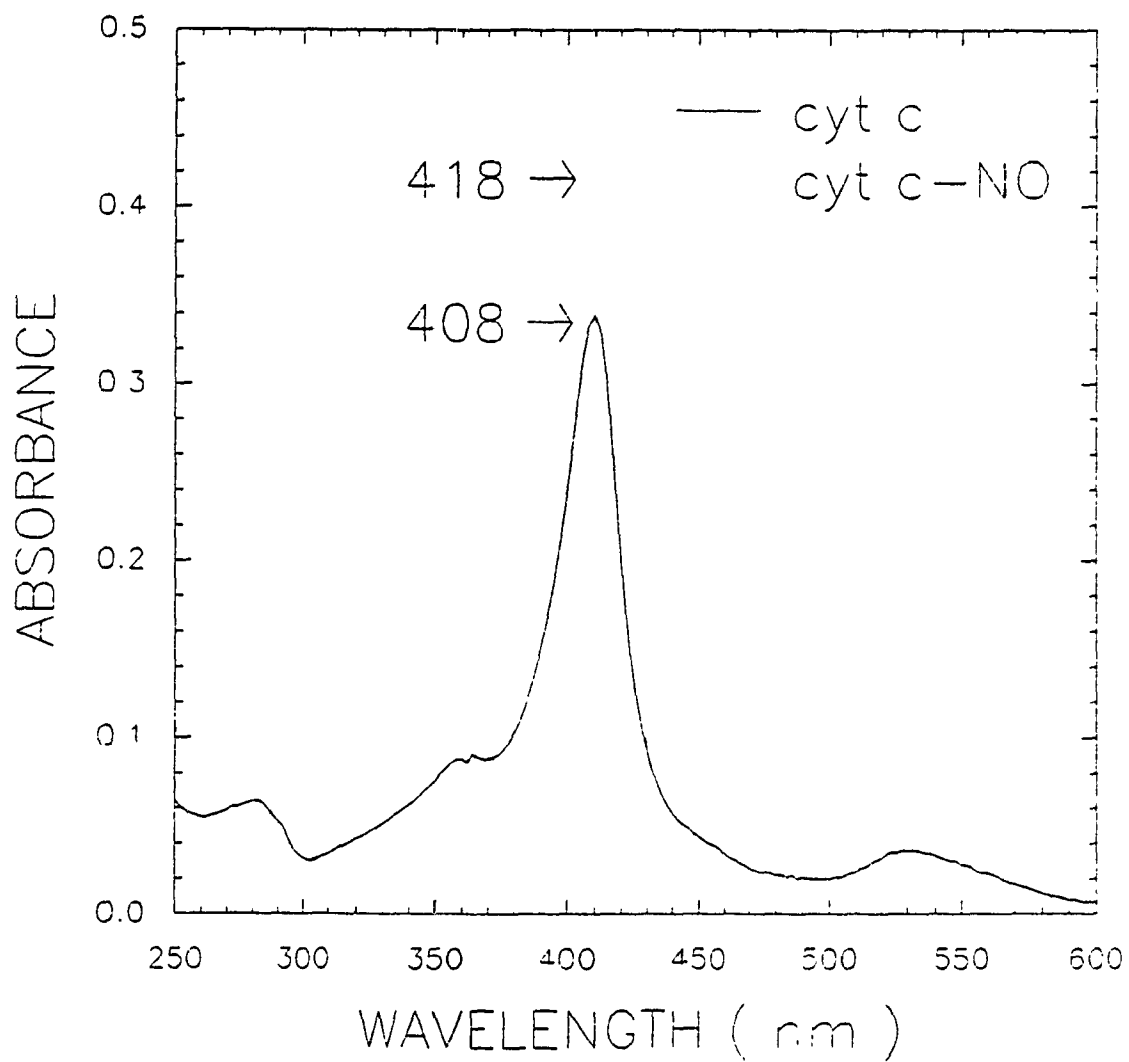
Figure 1.6. Absorption spectra of 3.2 μM cyt c(III) (solid line) and its NO adduct (dotted line) in 100 mM sodium phosphate, pH 7.0, 23 °C, 1-cm pathlength. [NO] = 100 μM
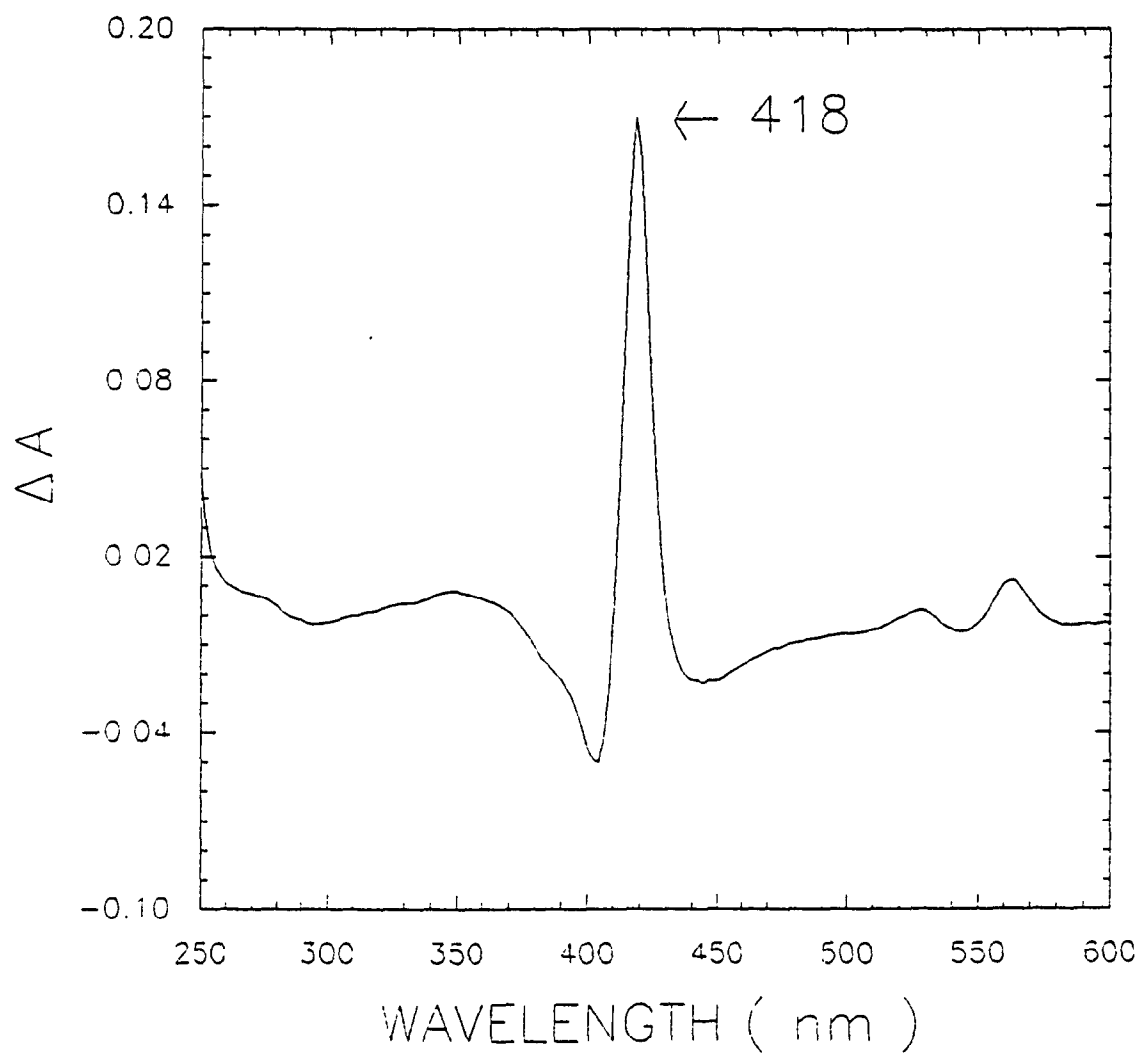
Figure 1.7. Difference spectrum between cyt c(III)-NO and cyt c(III).

Conditions as per Figure 1.6.
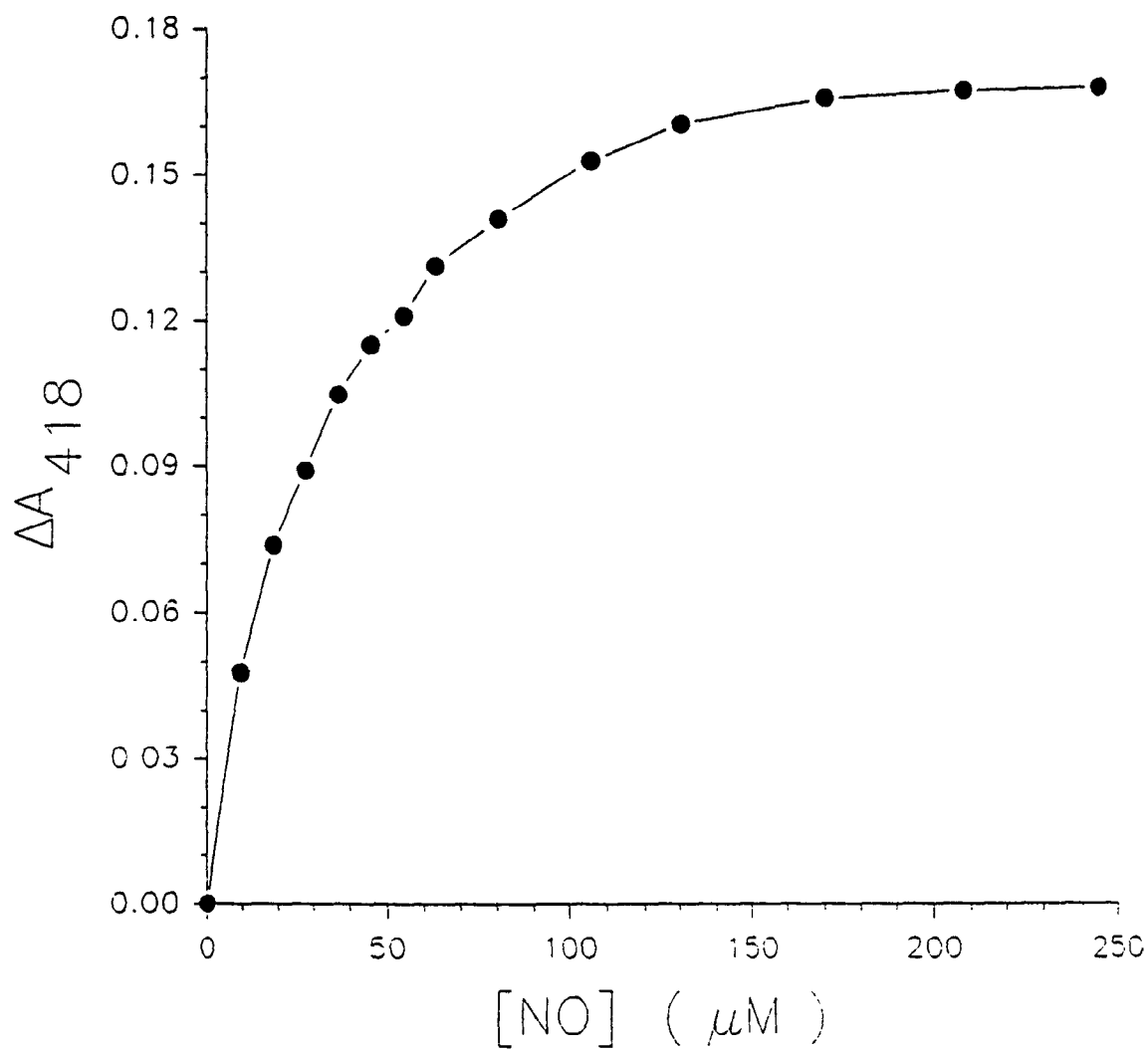
Figure 1.8. Spectrophotometric titration of 3.2 μM cyt c(III) at 418 nm with

NO in 100 mM sodium phosphate, pH 7.0, 23 °C.
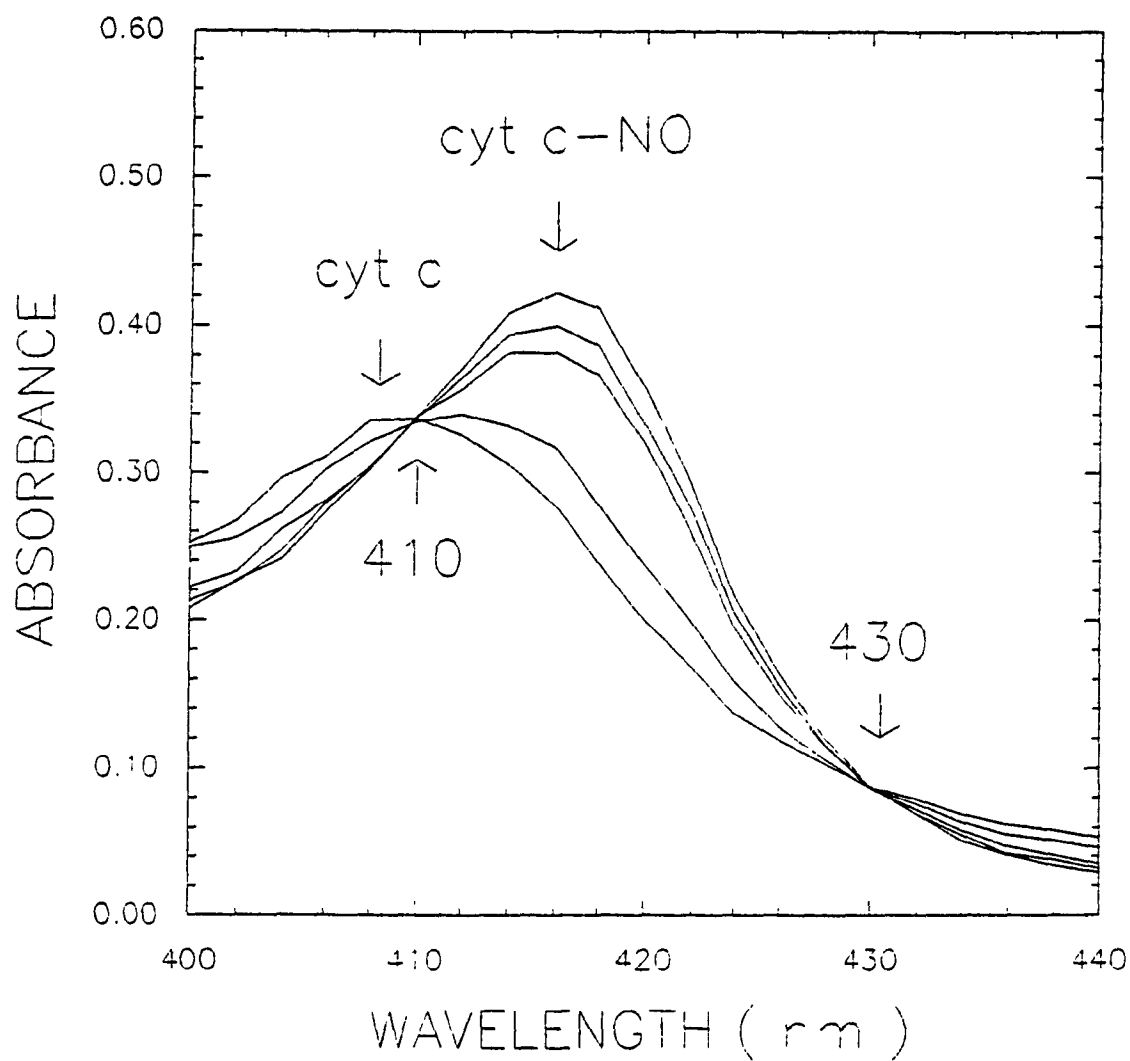
Figure 1.9. Overlay of spectra showing the conversion of free cyt c(III) to
cyt c(III)-NO during the titration of cyt c with NO. Conditions as
per Figure 1.8. Note the isosbestic points at 410 and 430 nm.
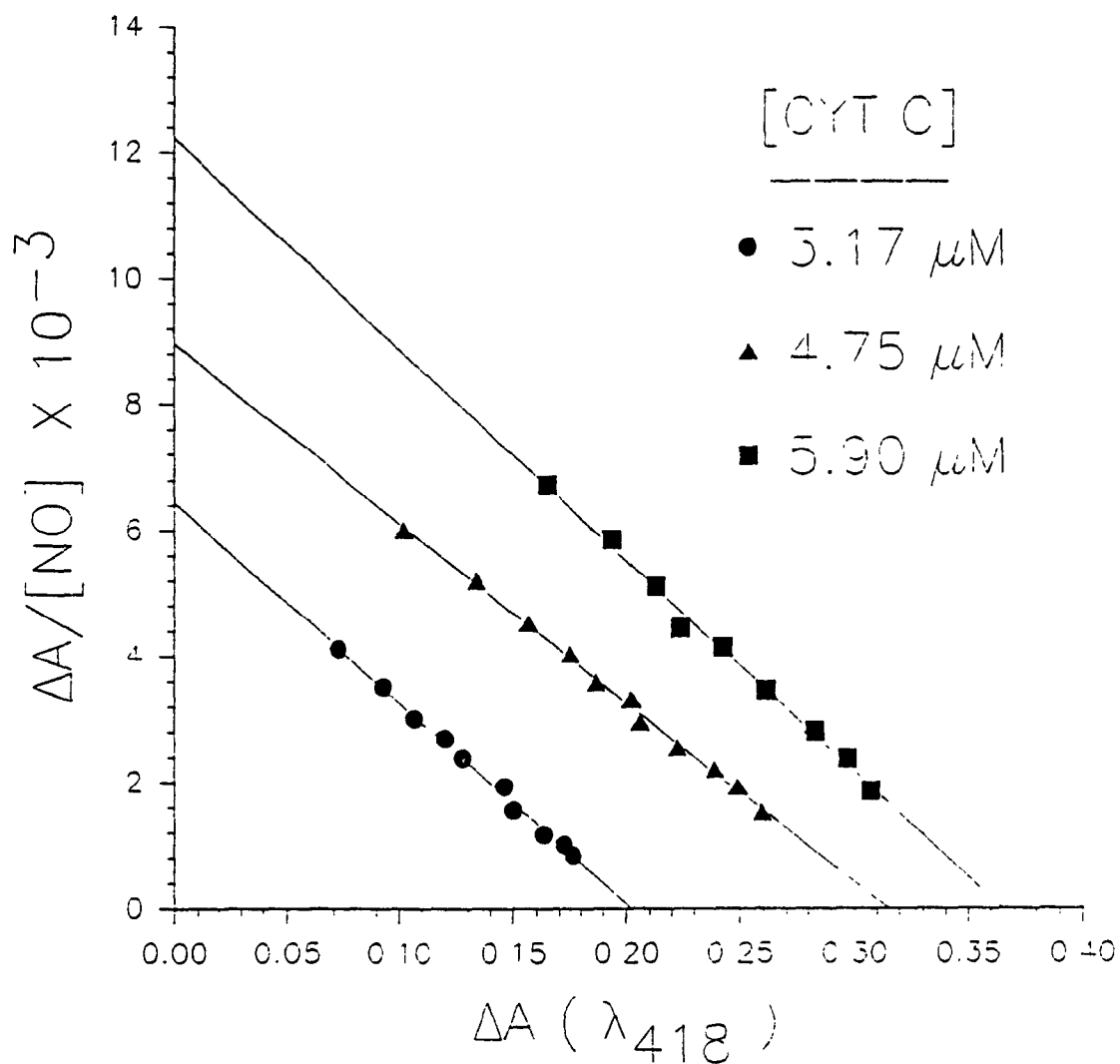
Figure 1.10. Scatchard plots for cyt c(III)-NO formation at various

concentrations of cyt c(III). Conditions as per Figure 1.8. Data

from Appendix B, Tables I-III.

Table 1.III. Equilibrium Dissociation Constants for The Binding of NO by

Cyt c(III) in 10 mM Sodium Phosphate Buffer, pH 7.0, 23 °C

[Cyt c] (μM)	K_D (μM)
3.17	34.5
4.75	39.7
5.90	34.6

1.43 Kinetic Determination of K_D for the Cyt c(III)-NO Complex.

Figure 1.11 shows typical reaction time courses with various concentrations of NO upon mixing cyt c(III) and NO in the stopped-flow instrument. A simple first order equation was fitted to the data using the Simplex nonlinear regression method [17]. A typical first order fit of the observed absorbance data is shown in Figure 1.12, and the observed rate constants (k_{obs}) at different [NO] are listed in Table 1.IV.

A plot of k_{obs} versus NO concentration gives a straight line with intercept equal to k_{off} and slope equal to k_{on} (Eq 1.8: $k_{obs} = k_{on} [NO]_T + k_{off}$). This plot is shown in Figure 1.13 and the values for k_{on} and k_{off} are 417 ± 60 M^{-1} s^{-1} and $0.027 \pm .004$ s^{-1}, respectively, and $K_D = 65 \pm 9$ μM.
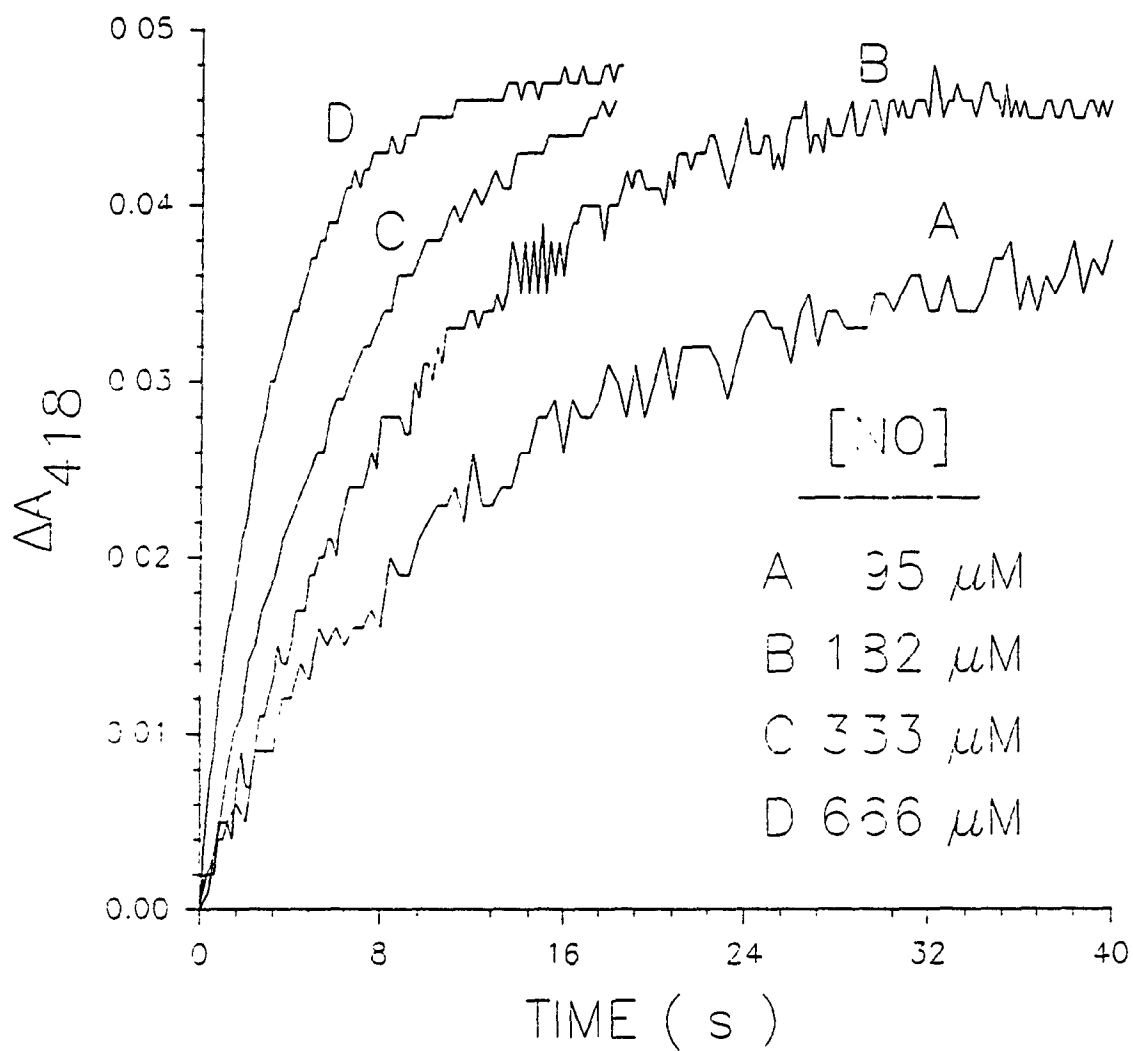
Figure 1.11. Reaction time courses for the reaction of various concentrations

of NO with 3.0-5.0 μM cyt c(III) in 10 mM sodium phosphate,
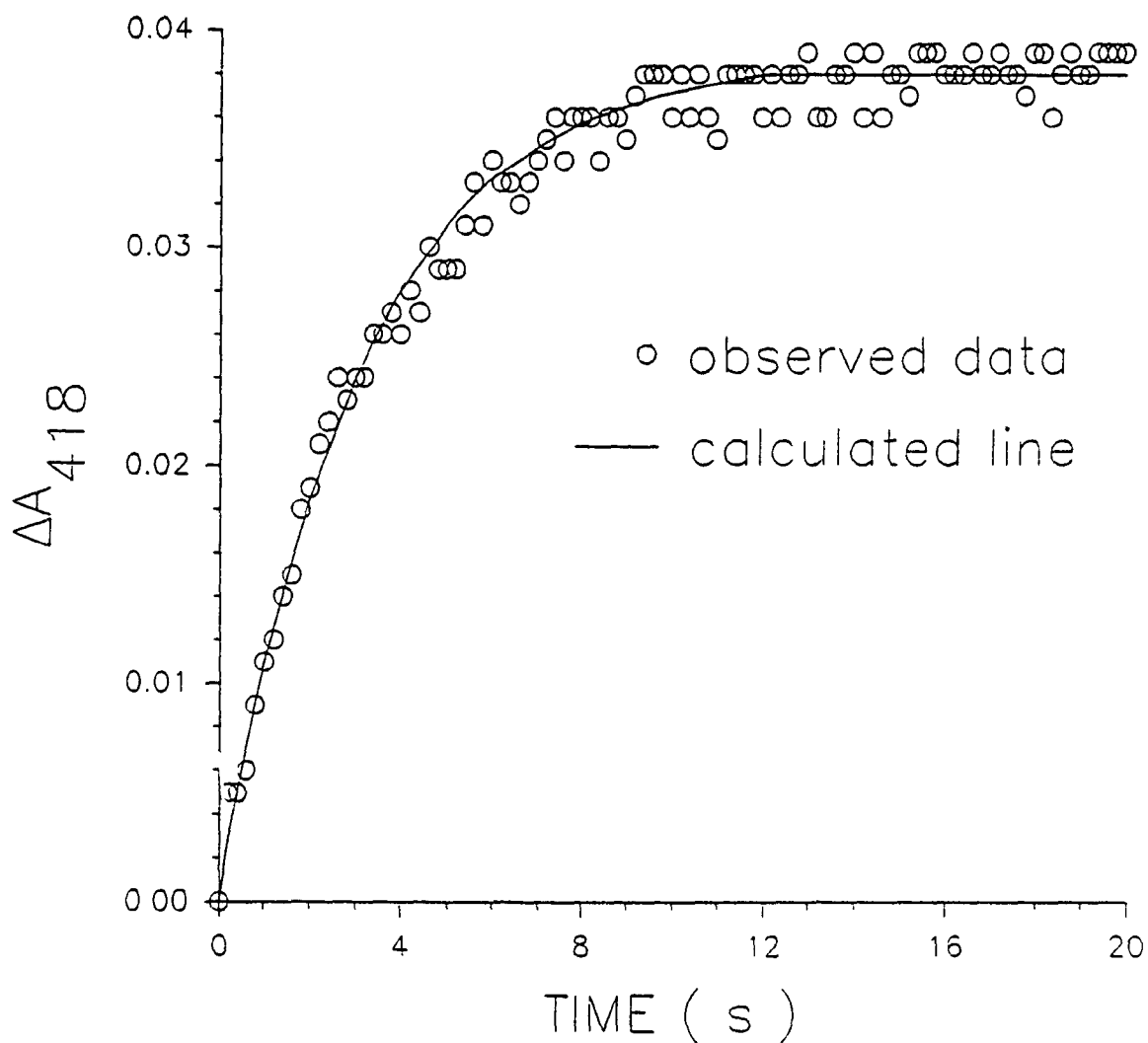
pH 7.0, 23 °C.

Figure 1.12. Reaction time course for the reaction of NO with 3.33 μM cyt

c(III) in 100 mM sodium phosphate, pH 7.0, 23 °C; [NO] = 666 μM.

The dots are the observed absorbance changes at 418 nm and the solid

line is a calculated first-order fit using the Simplex nonlinear

regression method (described in Data Analysis, Section 1.3).

Table 1.IV. Observed Rate Constants (k_{obs}) for The Binding of NO by

Cyt c(III) in 10 mM Phosphate Buffer pH 7.0, 23 °C

[NO] (μM)	k_{obs} (s^{-1})
95	0.07 ± 0.01
185	0.11 ± 0.02
333	0.15 ± 0.02
666	0.31 ± 0.04
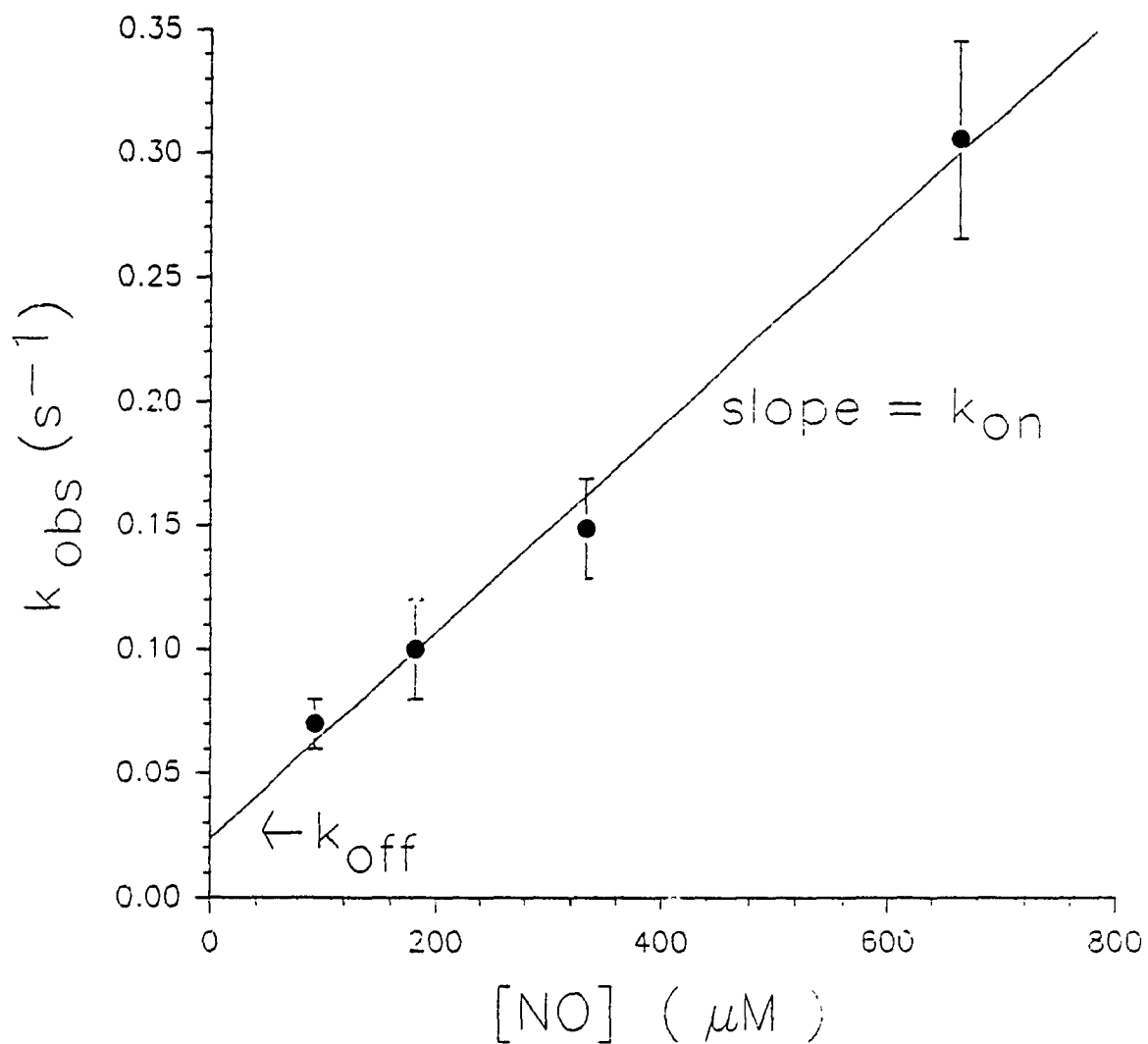
Figure 1.13. Plot of the observed rate constants versus [NO] for the reaction:

cyt c(III) + NO $\rightleftharpoons$ cyt c(III)-NO, in 10 mM sodium

phosphate, pH 7.0, 23 °C.
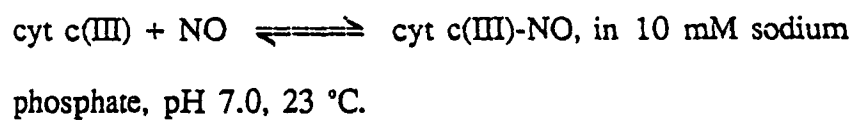
1.5 DISCUSSION

The equilibrium dissociation constants obtained here for the NO adducts of CCP(III) and cyt c(III) are summarized in Table 1.V. The similarity between the ratio of the kinetic constants (65 μM) and the equilibrium constant (36 μM), and the existence of a hyperbolic binding cur·e (Figure 1.8), for the binding of NO by cyt c(III), is consistent with a simple mechanism of ligand binding to a monomeric hemoprotein [1]:

$$P + NO \underset{k_{off}}{\overset{k_{on}}{\rightleftharpoons}} P\text{-}NO \tag{1.10}$$

The formation of CCP(III)-NO is also consistent with Eq 1.10, since its binding data corresponds to a hyperbolic curve (Figure 1.3). Therefore, the NO binding properties of cyt c(III) and CCP(III) can be compared.

Surprisingly, both CCP and cyt c have similar K_D's which indicates that both nitrosyl adducts have the same degree of stability. However, their heme environments are different; the heme of CCP is five coordinate [19] and is buried approximately 10 Å beneath the surface of the protein [20]. The heme of cyt c, on the other hand, is six coordinate and is situated in a hydrophobic cleft near the surface of the protein [7]. A comparison of the on and off rates between

Table 1.V. Equilibrium Dissociation Constants for the Binding to CCP
and Cyt C

Heme Protein	K_D (μM)	
	Equilibrium Determination	Kinetic Determination
CCP	44 ± 5	----
Cyt C	36 ± 3	65 ± 9

hemoproteins and NO, which are listed in Table 1.VI, should shed more light on these NO adducts.

Sharma et al. [9] have shown that the loss of H_2O from the sixth coordination site of ferric heme slows down NO-heme association rates. For example, the rate of NO binding by sperm whale Mb (6-coordination) is slower than elephant Mb (5-coordination) because the former reaction is rate-limited by the dissociation of H_2O from the six coordinate site. Therefore, one would expect CCP to react rapidly with NO because its sixth coordination site is free. On the other hand, one would expect NO binding to cyt c(III) to be slow since it is a ligand replacement reaction. The replacement of Met-80 by most ligands is rate-limited by the dissociation of the Fe(III)-Met bond at high ligand concentrations (also called crevice opening) [20a]:

SCHEME I
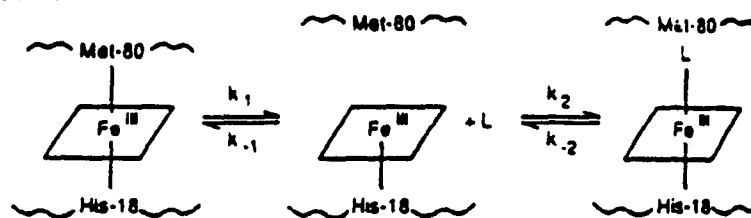
Table 1.VI. Rate Constants for the Combination of NO with Ferric Heme
Proteins

Heme Protein	k_{on} (M^{-1} s^{-1})	k_{off} (s^{-1})	Ref
Sperm whale Mb (6-coordinate)	5.3×10^4	14	15
Elephant Mb (5-coordinate)	2.2×10^7	40	15
Horseradish peroxidase (5-coordinate)	2×10^5	----	25
CCP (5-coordinate)	6.6×10^5	29[a]	this work
Cyt c (6-coordinate)	4.2×10^2	0.027	this work

[a] Estimated from the experimental $K_D = 44$ μM

NO must compete with sulphur of Met-80 for the sixth Fe coordination site. The k_{on} for the binding of NO by cyt c(III) is 417 M^{-1} s^{-1}, which is slow compared to 5- and even 6-coordinate proteins, since Met-80 dissociation from the Fe(III) atom is slow [20a].

The k_{on} for the reaction between CCP and NO has been determined previously [21] to be 6.6 X 10^5 M^{-1} s^{-1}. The on rate for CCP(III)-NO is fast and it is similar to that of 5-coordinate horseradish peroxidase. The difference between the peroxidase on-rates and that of elephant Mb is probably due to the fact that the hemes in the peroxidases are more buried than in Mb.

The off-rates for CCP(III)-NO and other NO adducts (except cyt c-NO) in Table 1.VI are very similar. These fast off-rates are probably due to increased proximal tension, following ligand binding, that destabilizes the adducts. The crystal structure of CCP(III)-NO [6] shows that the iron atom moves ≈ 0.2 Å towards the distal cavity on binding NO. This creates a strain on the bond formed between the proximal His-191 and the iron atom. Therefore, peroxidases may have fast NO off-rates because they prefer to be 5- as opposed to 6-coordinate. Also, the structure of the distal cavity may contribute to the fast off-rates since the NO ligand binds to the heme with bent geometry even though it prefers a linear geometry [6].

The off-rate for the cyt c(III)-NO is surprisingly slow. However, since cyt c is normally 6-coordinate, its heme cavity is better suited to accommodate a sixth

ligand (less proximal tension), and NO may be able to bind with a linear geometry (low energy). These factors may increase the stability of the NO adduct, and therefore, decrease the NO off-rate. Finally, ligand binding is clearly dependent on the location and structure of the heme pockets, and therefore, CCP and cyt c have similar K_D values only because the ratio (k_{off}/k_{on}) of their rate constants is similar.

These rate and equilibrium constants will be used in the following chapters to explain the rates and the products formed following mixing of the reagents below:

1. CCP(II)-NO + cyt c(III) ----------> ?

2. CCP(III) + cyt c(III) + NO ------> ?

CHAPTER 2

EFFECTS OF NITRIC OXIDE

COORDINATION

ON THE REDOX REACTIVITY OF

CYTOCHROME C PEROXIDASE

2.1 INTRODUCTION

One of the most intriguing factors that controls protein electron transfer rates is the nature of the protein matrix that intervenes between the donor and acceptor sites. Identification of the electron transfer pathway may shed some light on the mechanism of electron transfer. The CCP/cyt c complex is an obvious choice for such structure-function studies since the crystal structures of both CCP [5] and cyt c [7] are known to high resolution. Furthermore, recent studies have shown that intracomplex electron transfer occurs between CCP(II) and horse cyt c [22]:

$$CCP(II)/cyt\ c(III) \xrightleftharpoons{k_\alpha} CCP(III)/cyt\ c(II) \qquad (2.1)$$

$$\Delta E^\circ = 0.46\ V$$

where k_α is 0.22 s^{-1} in 10 mM sodium phosphate, at pH 7.0, and 24 °C.

Ligand binding studies are one of the most important tools for probing the active sites of hemoproteins. For example, valuable information about structure has been obtained by observing the effects of binding of CN^- [23], HF [24], and NO [25], to the heme of CCP. The binding of ligands to the iron atom of the protein can also be used to modify the redox reactivity of the heme.

The NO adducts of both CCP(II) and CCP(III) are stable [2]. Furthermore, the crystal structure of CCP(III)-NO [6] reveals that NO binding causes positional

adjustments of the heme iron and of some amino acid residues on the proximal and distal sides of the heme, as shown in Figure 2.1. The indole ring of Trp-51, Arg-48, and the imidazole ring of His-52 move 0.25 - 0.5 Å away from the heme ring, and the Fe(III) atom moves $\approx$ 0.2 Å directely into the plane of the heme. Therefore, the distance between the iron and the proximal His-175 increases from 2.0 Å in CCP to 2.2 Å in the NO adduct. The indole ring of Trp-191 moves 0.25 Å away from the imidazole of His-175, and Met-230 (located beneath Trp-191) moves 0.25 Å away from the indole ring of Trp-191. The orientation of these distal residues is important since they are located along the proposed electron transfer pathway between the hemes of CCP and cyt c [25a].

In this study, we investigate the effects of NO adduct formation on the redox reactivity of CCP by comparing the rates of electron transfer from CCP(II) and CCP(II)-NO to cyt c(III). Any changes in redox reactivity of CCP(II), however, will not be solely due to structural rearrangements since an increase in reduction potential, and a spin change from high to low spin is also observed following NO binding. The rate constant of interest is k'_α in the following reaction:

$$\text{CCP(II)-NO/cyt c(III)} \xrightleftharpoons{k'_\alpha} \text{CCP(III)-NO/cyt c(II)} \tag{2.2}$$

Finally, 3 different reductants, isopropyl alcohol, sodium dithionite, and rutheniumhexaammine(II), were used to reduce CCP(III) to CCP(II) in an attempt to minimize side reactions.
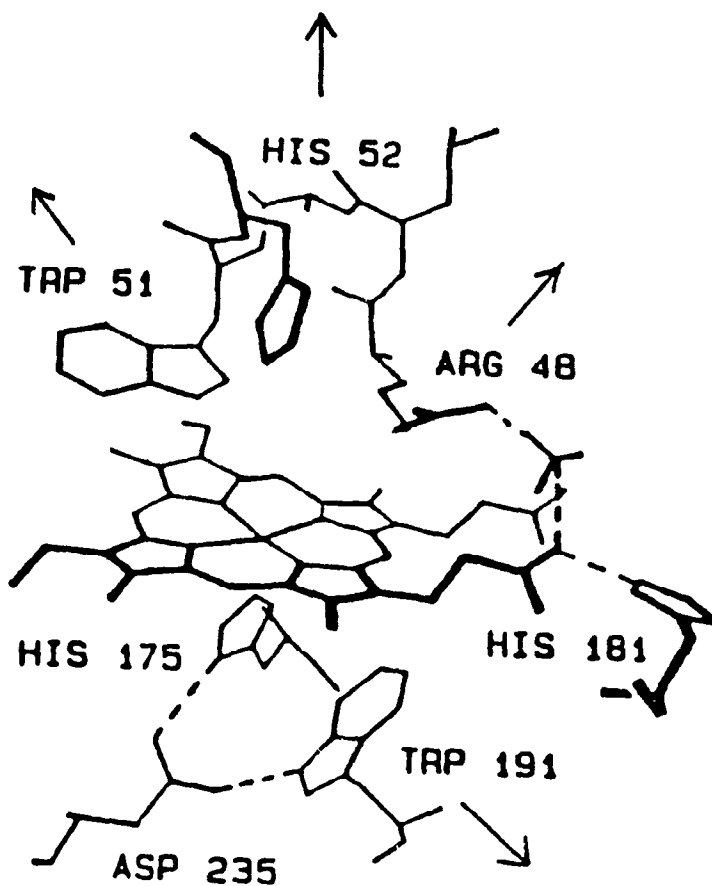
Figure 2.1. Heme crevice of CCP(III). The arrows indicate the direction of

the movement of the amino acid residues on binding NO to the

Fe(III) atom. Note that Trp-191 is located along the proposed

electron transfer pathway between the hemes of CCP and cyt c,

and Met-230 (not shown) is beneath Trp-191.

2.2 EXPERIMENTAL

MATERIALS-

Yeast CCP was isolated by the published procedure [12], and type VI horse heart cyt c was obtained from Sigma. The concentrations of CCP(III) and cyt c(III) were determined from their optical absorption spectra using extinction coefficients of 98 mM^{-1} cm^{-1} at 408 nm [13], and 106.1 mM^{-1} cm^{-1} at 410 nm [14], respectively. Nitric oxide (CP grade) was obtained from Union Carbide and was passed through KOH pellets before use to remove any higher oxides of nitrogen. Isopropyl alcohol (HPLC grade), acetophenone, sodium dithionite, and rutheniumhexaammine(III) chloride were purchased from Fisher, May and Baker, Aldrich, and Strem chemical, respectively.

METHODS-

All investigations were performed with a CCP(III) concentration of $\approx$ 3 μM in 10 mM sodium phosphate, pH 7.0, 23 °C. The reduction of CCP(III) was carried out using one of the following reducing agents: (1) isopropyl alcohol radicals, (2) sodium dithionite, and (3) rutheniumhexaammine(II). The procedures used to investigate rx 2.2 depended on the reducing agent used and are outlined under separate headings.

2.2.1. Reduction of CCP(III) by Isopropyl Alcohol Radicals:

CCP crystals were dissolved in 2.0 mL of 10 mM sodium phosphate buffer containing 0.008% acetophenone and 2% isopropyl alcohol in a 1-cm cuvette and degassed by bubbling argon into the protein solution for at least one hour. CCP(II) was formed in situ by UV-irradiation [26]. The photoreduction was monitored by changes in the Soret region as shown in Figure 2.2. Once reduction was complete, 10 µL of NO-saturated buffer ($\approx$ 2 mM NO) were added to the cuvette using a gas-tight syringe to form CCP(II)-NO, which was identified by its Soret maximum at 424 nm as shown in Figure 2.3.

Once CCP(II)-NO was formed, $\approx$ 30 µL of deoxygenated cyt c(III) were injected into the cuvette to give a final cyt c concentration of 3.0 µM. The sample was rapidly mixed and the reaction was followed at 414 nm using a rapid response spectrophotometer (HP Model 8451 A). At the monitoring wavelength, a maximum absorbance change of $\approx$ 0.2 was expected due to (1) the reduction of cyt c(III) (ΔA $\approx$ 0.1) as calculated from $\Delta\varepsilon$ (red-ox) = 34 mM^{-1} cm^{-1} for cyt c at 415 nm [14], and (2) oxidation of CCP(II)-NO to CCP(III)-NO (ΔA $\approx$ 0.1) (Figure 2.3). Since 414 nm is an isobestic point in the spectra of CCP(III) and CCP(III)-NO (see Figure 1.4 in Chapter 1), the same ΔA at 414 nm should be observed weather CCP(III) or its NO adduct results from oxidation of CCP(II)-NO.
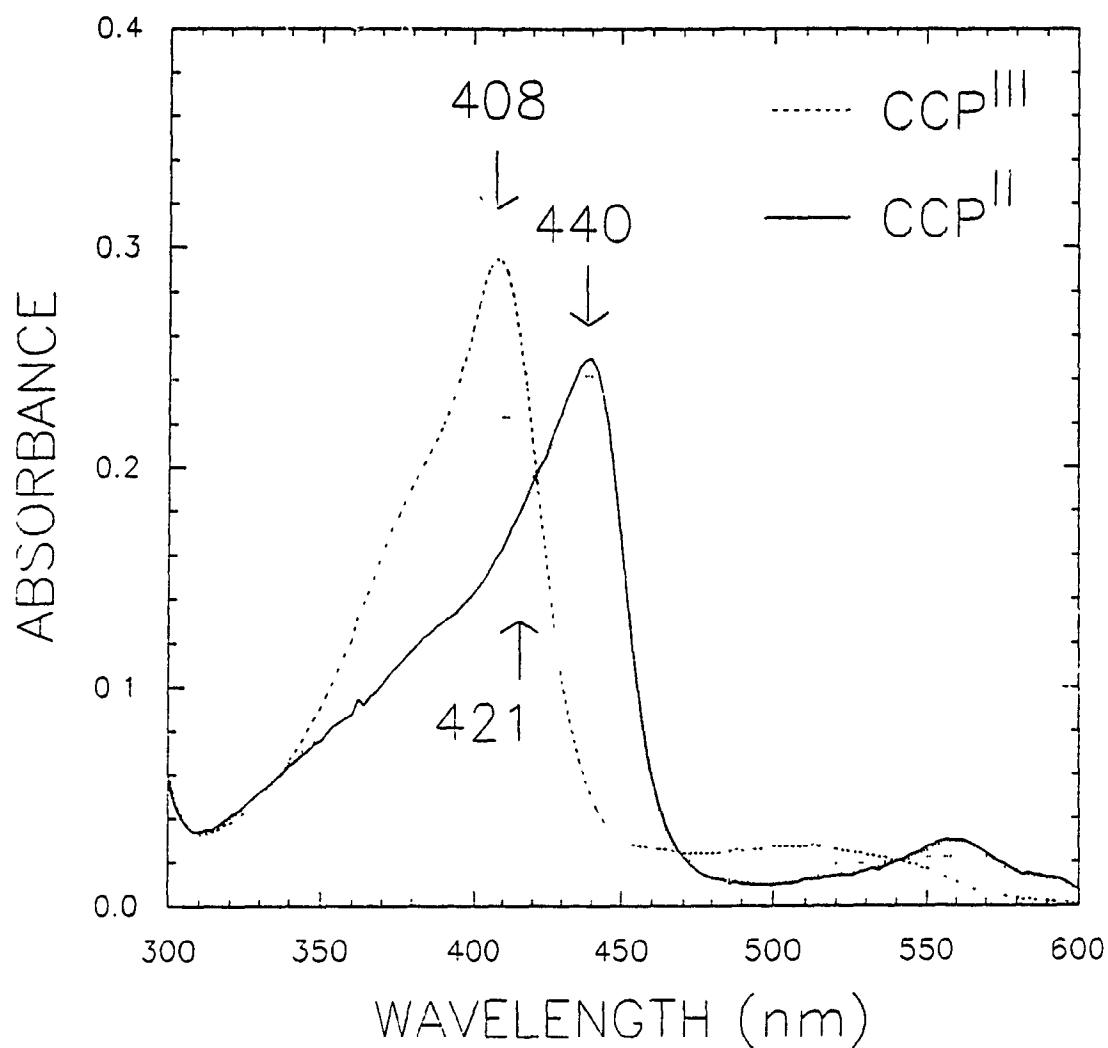
Figure 2.2. Absorption spectra showing the conversion of 3.0 μM CCP(III)

(λ_{max} = 408 nm) to CCP(II) (λ_{max} = 440 nm) by isopropyl alcohol

radicals in 10 mM sodium phosphate, pH 7.0, 23 °C. Note the

isosbestic point at 421 nm.
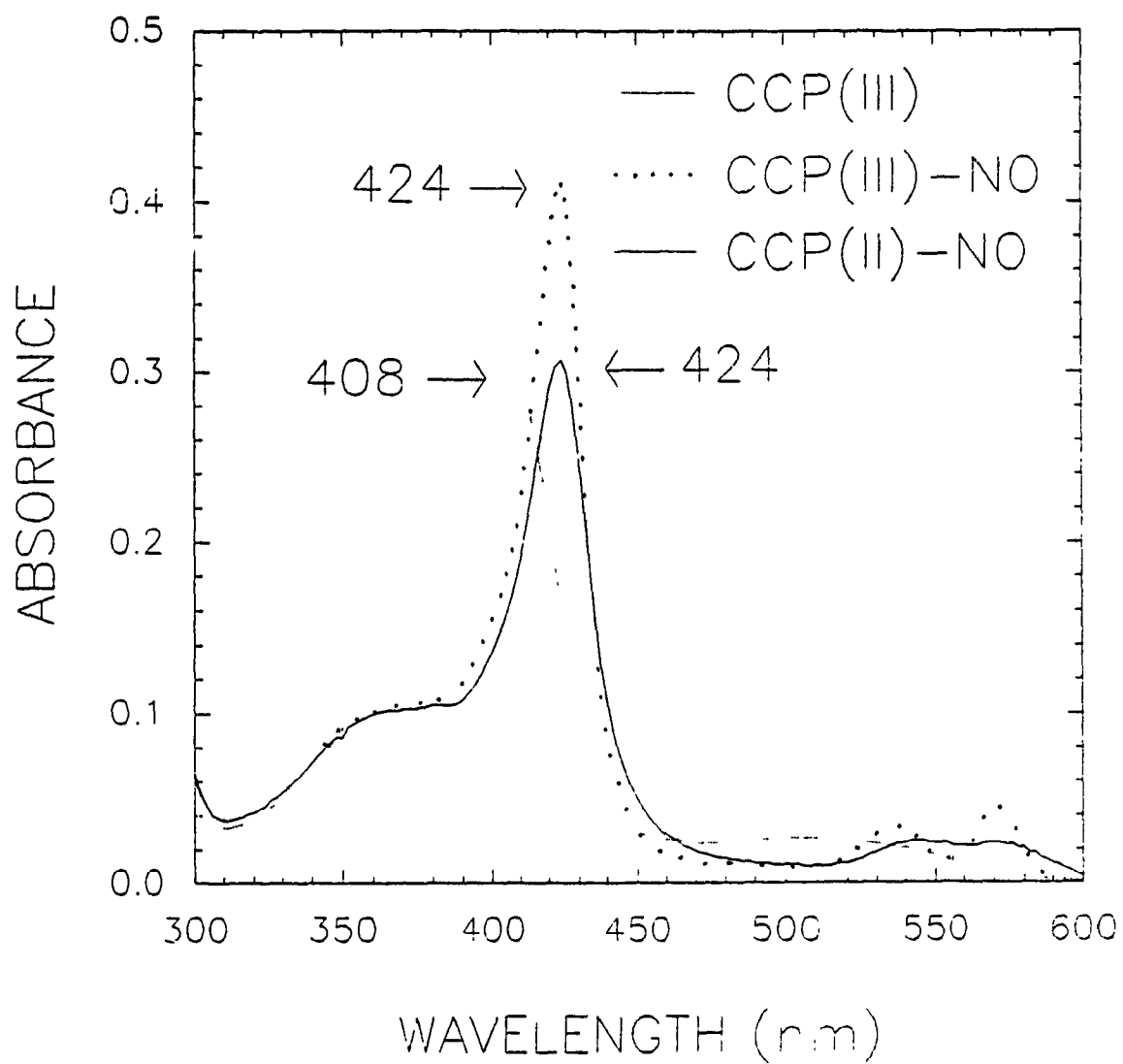
Figure 2.3. Absorption spectra of CCP(III) (dashed line), CCP(III)-NO
(dotted line), and CCP(II)-NO (solid line). Conditions as per
Figure 2.2.

2.2.2. Reduction of CCP(III) by Sodium Dithionite:

These reactions were carried out as described above except that CCP(III) was reduced with sodium dithionite. CCP(III) crystals were dissolved in 2.0 mL of 10 mM phosphate buffer in a 1-cm cuvette, and degassed with argon for at least one hour. 1-2 μL of a concentrated solution of dithionite were then added, using a gas-tight syringe, until CCP(III) was completely reduced.

2.2.3. Reduction of CCP(III)-NO by Rutheniumhexaammine(II):

Rutheniumhexaammine(II) was prepared by dissolving a known amount of Ru(III) in water and deoxygenating for $\approx$ 30 min in the presence of amalgamated zinc.

These reactions were carried out as described in Section 2.2.1 above except that 21 μM rutheniumhexaammine(II) was added to 3.0 μM CCP(III) and 10 μM NO. Enough cyt c ($\approx$ 27 μM) was then added to the reaction mixture to oxidize the excess Ru(II) and CCP(II)-NO. Cyt c(III) reduction was monitored at 550 nm because the absorbance in the Soret region of the reaction mixture was too high due to the excess cyt c present. At this wavelength, a maximum absorbance change of $\approx$ 0.48 was expected due to (1) the reduction of cyt c(III) ($\Delta A \approx 0.46$) as calculated from $\Delta\varepsilon$ (red-ox) = 19 mM^{-1} cm^{-1} for cyt c at 550 nm [14], and (2) oxidation of CCP(II)-NO to CCP(III)-NO ($\Delta A \approx 0.02$) (Figure 2.3).

2.3 DATA ANALYSES

All kinetic data were analyzed by the Simplex nonlinear regression method [17] (see Section 1.3: Data Analyses in Chapter 1).

2.4 RESULTS

The effect of NO coordination on the redox reactivity of CCP(II) was investigated by measuring the absorbance growth at 414 and 550 nm, following mixing of CCP(II)-NO and cyt c(III). Three different reducing agents were used to reduce CCP(III), and the results are discussed separately for each reductant.

2.4.1. Reduction of CCP(III) by Isopropyl Alcohol Radicals:

Figure 2.4 shows the observed absorbance growth at 414 nm following mixing of 3.0 μM CCP(II)-NO and 3.0 μM cyt c(III). A simple first-order equation was fitted to the growth which yields a rate constant of 0.005 s-1. The maximum observed change (ΔA = 0.08) represents $\approx$ 40% of the calculated change at 414 nm. The products of this reaction were examined by subtracting the absorbance contribution of 3.0 μM cyt c(II) from the product spectrum. An overlay of the product spectrum and that of 3.0 μM cyt c(II) is given in Figure 2.5. The spectrum in Figure 2.6 obtained following subtraction of cyt c(II) is identical to that of $\approx$ 3.0 μM CCP(III). Clearly, CCP(II)-NO was oxidized and cyt c(III) was reduced. Therefore, k_{obs} could possibly correspond to the rate constant for intramolecular electron transfer from CCP(II)-NO to cyt c(III):

$$\text{CCP(II)-NO/cyt c(III)} \overset{k_{obs}}{\rightleftharpoons} \text{CCP(III)/cyt c(II) + NO} \qquad (2.3)$$

Figure 2.4. Reaction time course following rapid mixing of 3.0 µM

CCP(II)-NO and 3.0 µM cyt c(III) at λ_{414} in 10 mM sodium

phosphate, pH 7.0, 23 °C. Isopropyl alcohol radicals were used to

reduce CCP(III) to CCP(II). The solid line is the calculated

first-order fit using the Simplex nonlinear regression method which

yields $k_{obs} = 0.005$ s^{-1}.
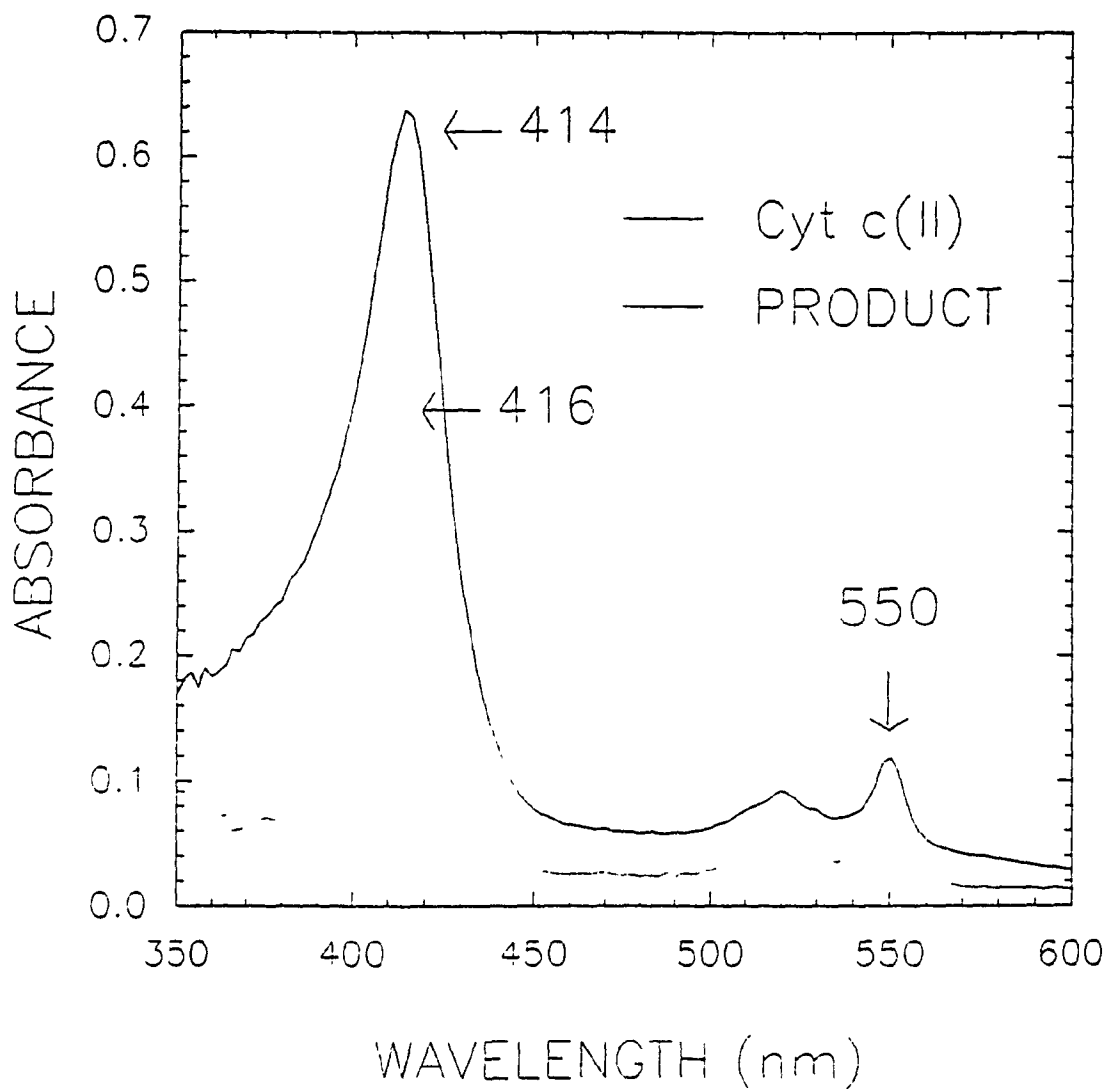
Figure 2.5. Absorption spectra of 3.0 μM cyt c(II) (dotted line) and of the products (solid line) following mixing of CCP(II)-NO and cyt c(III) in 10 mM sodium phosphate, pH 7.0, 23 °C.
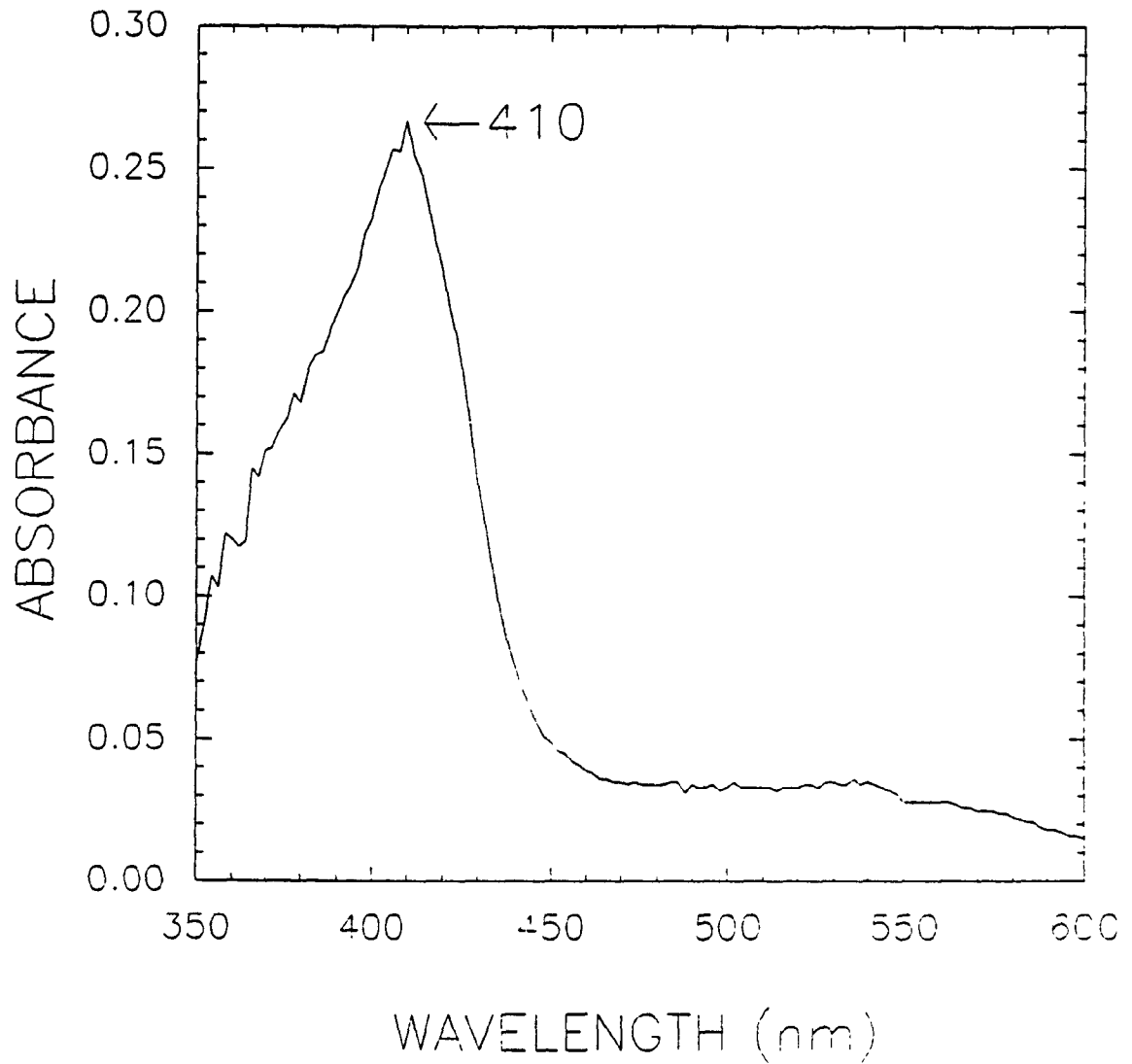
Figure 2.6. Product absorption spectrum shown in Figure 2.5 minus the

spectrum of 3.0 µM cyt c(II). Note that the spectrum resembles

that of ≈ 3.0 µM CCP(III). Conditions as per Figure 2.5.

Other reactions may also contribute to the absorbance change at 414 nm shown in Figure 2.4. For example, slow reduction of cyt c(III) was observed in the absence of CCP(II)-NO. A 3.0 μM solution of cyt c(III) in photochemical buffer was irradiated under the same conditions that were used to reduce CCP(III), and instantaneous reduction of cyt c(III) was observed. Next, a second aliquot of cyt c(III) was added to the reaction mixture to give a final concentration of 6.0 μM cyt c(III). Slow reduction of cyt c(III) was observed, and a simple first-order equation was fitted to the absorbance growth ($\Delta A \approx 0.035$) which yields a rate constant of 0.0014 ± 0.0007 s^{-1}. This indicates that long-lived reducing species are formed in excess during irradiation.

Also, binding of NO by cyt c(III) gives rise to an absorbance growth ($\Delta A \approx 0.02$) at 414 nm. The second-order rate constant for rx 2.4 is 417 M^{-1} s^{-1} (Table VI in Chapter 1):

$$\text{cyt c(III) + NO} \overset{k}{\rightleftharpoons} \text{cyt c(III)-NO} \qquad (2.4)$$
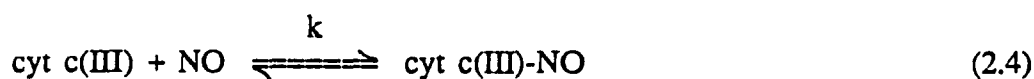
However, k in Eq 2.4 is probably reduced in the presence of CCP(II)-NO since in Chapter 3 it is shown that binding of CCP(III)-NO reduces k to 305 M^{-1} s^{-1}. Therefore, under the present experimental conditions [7.0 μM NO (10 μM - the amount bound to 3.0 μM CCP) and 3.0 μM cyt c(III)], the bimolecular rate of formation of cyt c(III)-NO is expected to be slow relative to $k_{obs} = 0.005$ s^{-1}.

Also, since the K_D for cyt c(III)-NO is $\approx$ 40 μM (Table 1.V), the contribution of this adduct, at 7.0 μM NO, to the final product spectrum shown in Figure 2.5 will be small.

Finally, in the absence of cyt c(III), 50-100% of CCP(II)-NO decays to CCP(III) and this gives rise to an absorbance growth ($\Delta A_{max} \approx$ 0.03) at 414 nm with $k_{obs} \approx$ 0.006 s^{-1} if CCP(II) is generated using isopropyl alcohol radicals. This decay could explain the existence of CCP(III) in the product spectrum.

Therefore, the observed absorbance growth following mixing of CCP(II)-NO and cyt c(III) (Figure 2.4) can not be solely attributed to rx 2.3. Nonetheless, a limiting rate of $\leq$ 0.005 s^{-1} can be assigned to the rate of intramolecular electron transfer from CCP(II)-NO to cyt c(III).

2.4.2. Reduction of CCP(III) by Sodium dithionite:

Figure 2.7 shows the observed absorbance growth at 414 nm following mixing of 3.0 μM CCP(II)-NO and 4.0 μM cyt c(III). A simple first-order equation was fitted to the observed growth, and yields a rate constant of 0.006 s^{-1}. The maximum absorbance change (ΔA=.08) represents $\approx$ 40 % of the calculated change at 414 nm. Again, reactions other than electron transfer (rx 2.3) may contribute to the observed absorbance growth at 414 nm shown in Figure 2.7. For example, slow reduction of cyt c(III) was observed, in the absence of CCP(II)-NO, when a second
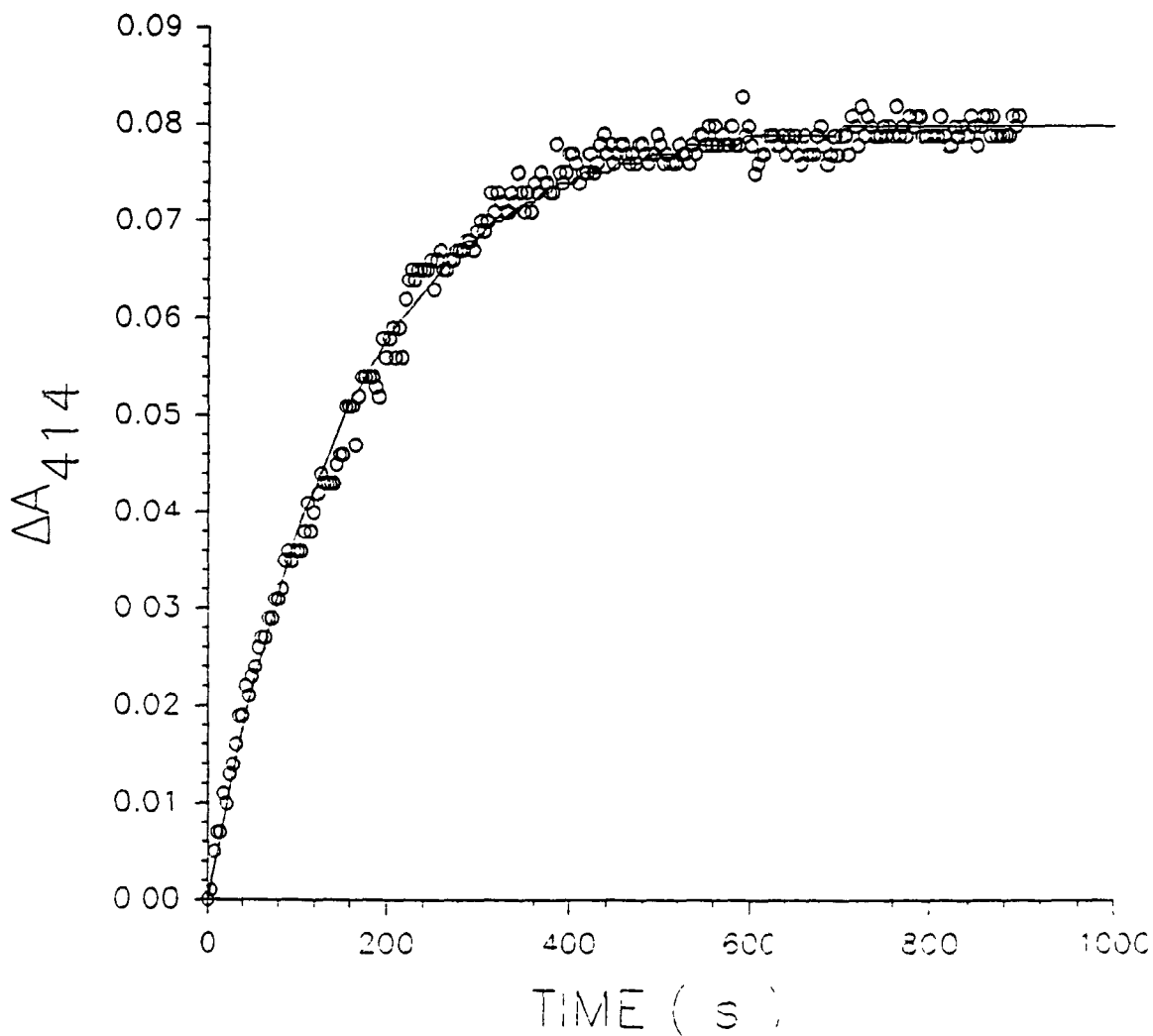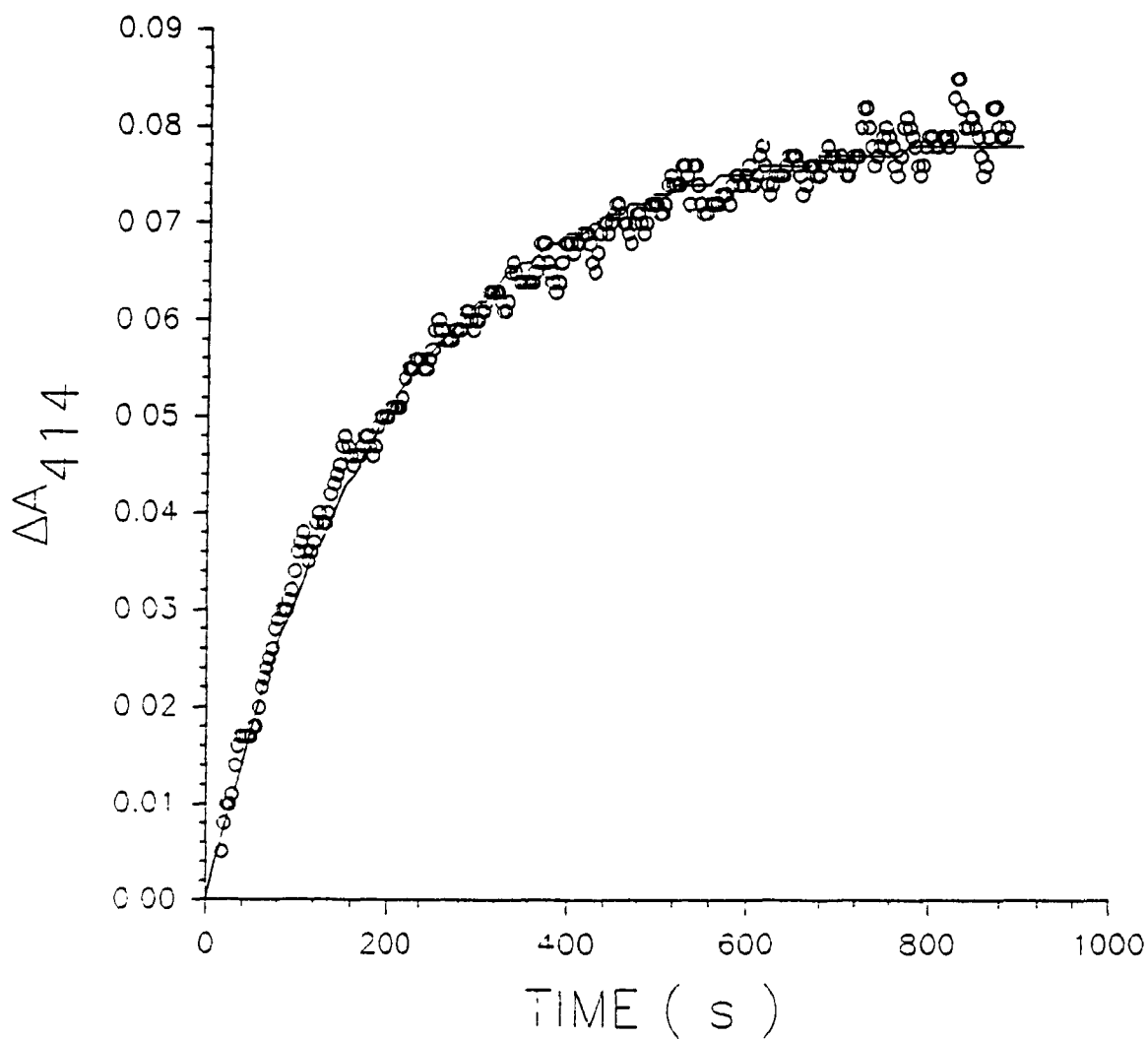
Figure 2.7. Reaction time course following rapid mixing of 3.0 μM

CCP(II)-NO and 4.0 μM cyt c(III) at λ_{414} in 10 mM sodium

phosphate, pH 7.0, 23 °C. Sodium dithionite was used to reduce

CCP(III). The solid line is a calculated first-order fit using the Simplex

nonlinear regression method which yields k_{obs} = 0.006 s^{-1}.

aliquot of cyt c(III) was added to a solution of cyt c(II) that had already been reduced by titration with dithionite. A simple first-order equation was fitted to the absorbance growth ($\Delta A \approx 0.05$) for this reduction which yields a rate constant of 0.004 ± 0.002 s^{-1}. This indicates again that reducing species are present in excess following CCP(III) reduction. Also, CCP(II)-NO decays and binding of NO by cyt c(III) could give rise to an absorbance at 414 nm (see Section 2.4.1 above).

2.4.3. Reduction of CCP(III)-NO by Rutheniumhexaammine(II):

At 10 µM Ru(II) and 10 µM NO the production of CCP(II)-NO took $\approx$ 2 h. Therefore, in order to form CCP(II)-NO within a reasonable time (5-10 min), the Ru(II) concentration was increased to 21 µM and enough cyt c(III) ($\approx$ 27 µM) was added to the reaction mixture to oxidize the excess Ru(II). Since Ru(II) reduces cyt c(III) in a rapid bimolecular reaction (6.7 X 10^4 M^{-1} s^{-1} [27]), the observed growth (Figure 2.8), following manual mixing (1-2 s), should not be due to cyt c(III) reduction by Ru(II). However, following mixing of 27 µM cyt c(III), 21 µM Ru(II), and 10 µM NO, in the absence of CCP(II)-NO, a growth at 550 nm was observed with $\Delta A \approx 0.07$. Furthermore, a linear growth at 550 nm with $\Delta A \approx 0.02$ was observed following mixing of 27 µM cyt c(III) and 10 µM NO.

Rapid mixing of 3.0 µM CCP(II)-NO, 27 µM cyt c(III), and 21 µM Ru(II) gave the absorbance growth at 550 nm shown in Figure 2.8. Its biphasic appearance clearly indicates that two or more processes are contributing to this absorbance

growth. A simple first-order equation was fitted to the growth for the first 900 s using the Simplex nonlinear regression method [17], and the observed rate constant (k_{obs}) is 0.004 s^{-1}. The second phase appears to be a linear growth. The initial observed growth ($\leq$ 900 s), therefore, could be due to cyt c(III) reduction since the rate of reduction of cyt c(III) is probably decreased in the presence of CCP (this is discussed in Chapter 3), and the second phase is possibly binding of NO by excess cyt c(III).
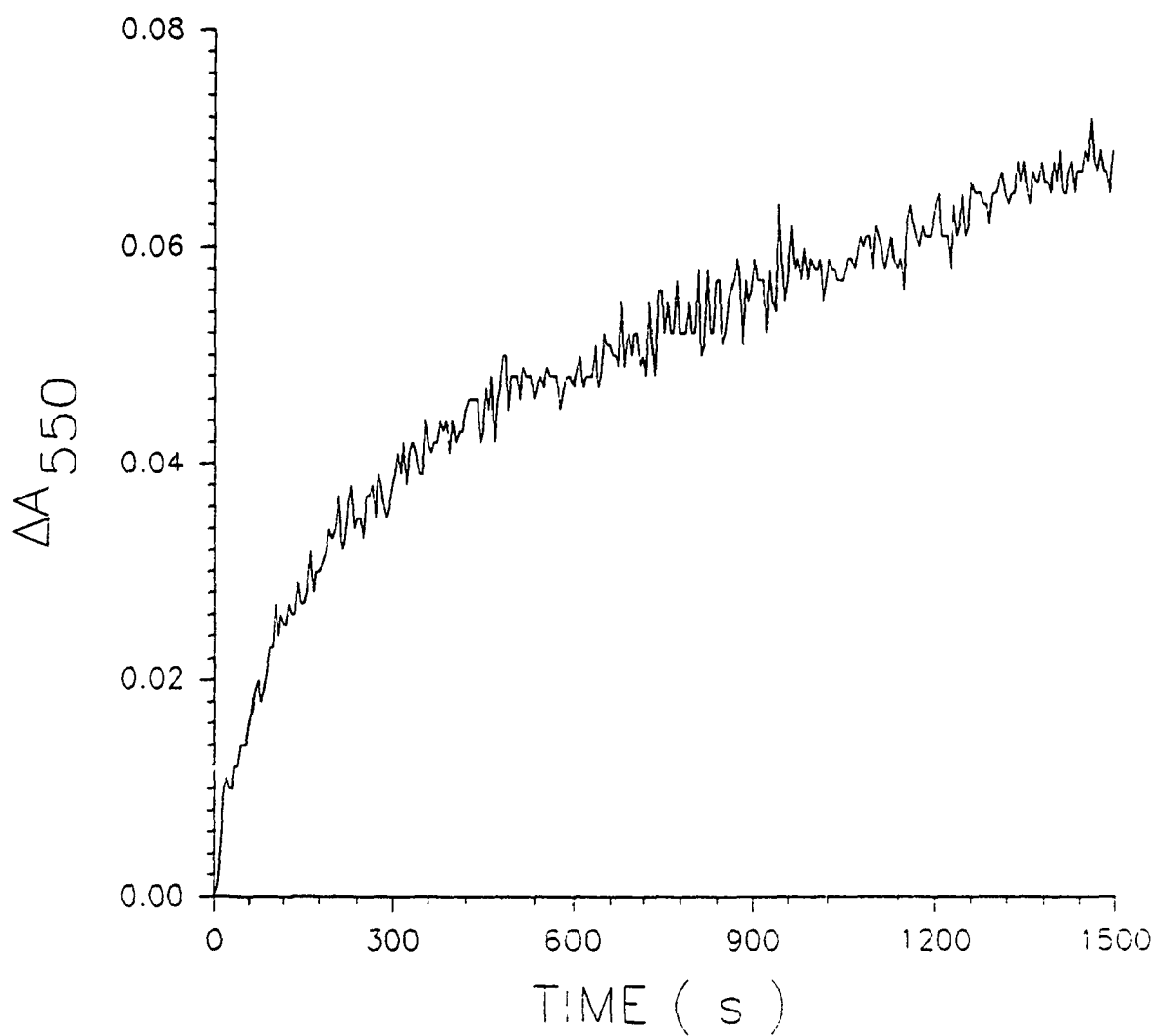
Figure 2.8. Reaction time course following rapid mixing of 3.0 μM

CCP(II)-NO and 27.0 μM cyt c(III) at λ_{550} in 10 mM sodium

phosphate containing 21 μM rutheniumhexaammine(II), pH 7.0,

23 °C.

2.5 DISCUSSION

The rates of electron transfer from CCP(II) to cyt c(III), in the presence and absence of NO, are ≤ 0.005 s^{-1} and 0.22 s^{-1} [22] respectively. These rate constants were determined following reduction of CCP(III) by isopropyl alcohol radicals in 10 mM sodium phosphate. In the absence of NO, the rate of electron transfer between CCP(II) and cyt c(III) can be determined accurately since this rate is > 35 fold faster than any of the observed side reactions. In the presence of NO, however, the observed reaction following mixing of CCP(II)-NO and cyt c(III) is very slow, so side reactions may contribute to the absorbance growth at 414 nm, as outlined in Section 2.4.1 of the Results.

Cyt c(II) and CCP(III) are the observed products when CCP(II)-NO and cyt c(III) are mixed following photochemical reduction of CCP(III). The presence of cyt c(II) in the product can be explained by reduction of cyt c(III) by long-lived reducing species, and/or by CCP(II)-NO. The presence of CCP(III) as a product may be due to oxidation of CCP(II)-NO via direct electron transfer to cyt c(III) or to radical-induced decay of CCP(II)-NO. Under the conditions of these experiments (NO = 7 μM), CCP(III) would be observed as a final product if CCP(II)-NO were oxidized since $K_D = 44 \pm 5$ μM for CCP(III)-NO (Table 1.V, Chapter 1).

Isopropyl alcohol radicals were replaced as the reducing agent by sodium dithionite in an attempt to minimize unwanted cyt c(III) reduction and

CCP(II)-NO decay. Sodium dithionite rapidly reduces cyt c(III) in a rapid bimolecular reaction (1.17×10^4 M^{-1} s^{-1} [28]), and thus, the observed absorbance growth at 414 nm can not be due to cyt c(III) reduction by dithionite. However, in the absence of CCP(II)-NO, slow reduction of a second aliquot of cyt c(III) was observed at 414 nm as outlined in Section 2.4.2 of the Results, and CCP(II)-NO also decayed in the presence of dithionite. Thus, side reactions may again contribute to the observed absorbance growth at 414 nm following mixing of CCP(II)-NO and cyt c(III) when dithionite was used to reduce CCP(III).

Next, rutheniumhexaammine(II) was employed as the reducing agent. Ru(II) is a one electron reductant and the Ru(III)/(II) reduction potential is 67 mV [29]. It was hoped that Ru(II) would stoichiometrically reduce CCP(III)-NO by the scheme below, and thus, eliminate unwanted cyt c(III) reduction and CCP(II)-NO decay:

$$CCP(III) + NO \; \underset{K}{\rightleftharpoons} \; CCP(III)\text{-}NO \qquad (2.8)$$

$$CCP(III)\text{-}NO + Ru(II) \; \longrightarrow \; CCP(II)\text{-}NO + Ru(III) \qquad (2.9)$$
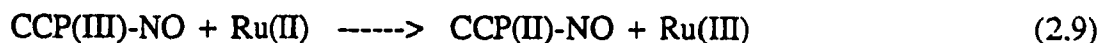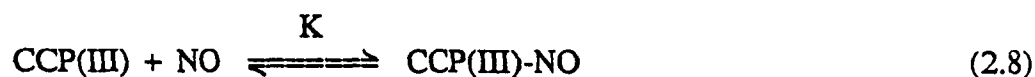
The reduction potential for the Fe(III)/Fe(II) couple of CCP is -194 mV [30]; however, ΔE° must increase when CCP binds NO since the Fe(II)-NO adduct of CCP is more stable than the Fe(III)-NO adduct. Furthermore, since CCP(II)-NO is produced following mixing of CCP(III)-NO and Ru(II), the E° of CCP must have increased by at least 250 mV on binding NO.

The observed absorbance growth at 550 nm following mixing of CCP(II)-NO and cyt c(III) (Figure 2.8) is biphasic and may again be due to a combination of cyt c(III) reduction by small molecules, binding of NO by cyt c(III), and electron transfer from CCP(II)-NO to cyt c(III). However, a simple first-order equation can be fitted to the first 900 s of the trace in Figure 2.8 with $k_{obs} = 0.004s^{-1}$.

In summary, similar first-order rates (0.005 s^{-1}) were observed when CCP(II)-NO and cyt c(III) were mixed using all three reductants. The rate of electron transfer from CCP(II)-NO to cyt c(III) is > 40 times slower than that from CCP(II) to cyt c(III). The decrease in the redox reactivity of CCP(II)-NO with cyt c(III) may be due in part to repositioning of Trp-191 when NO binds to CCP, since Trp-191 is located along the proposed electron transfer pathway between the hemes of CCP and cyt c. However, since CCP(III)-NO is reduced by Ru(II) (E° ≈ 67 mV), E° for the Fe(III)/(II) couple of CCP must increase by 250-300 mV on binding NO. Consequently, the driving force for electron transfer from CCP(II)-NO to cyt c(III) is decreased, and this may also account for the drop in the rate of electron transfer between CCP(II)-NO and cyt c(III). Finally, the high to low spin state conversion of the heme of CCP, which is observed when NO binds to CCP(III), may also contribute to the observed kinetics, however, the effect of spin states on protein electron transfer is not known.

CHAPTER 3

KINETIC PROBE OF HEME

ACCESSIBILITY OF

CYTOCHROMES C

IN COMPLEXES WITH

CYTOCHROME C PEROXIDASE

3.1 INTRODUCTION

Many studies have demonstrated rapid noncovalent complex formation between CCP(III) and cyt c(III). The association between the two proteins is largely electrostatic, as demonstrated by the large ionic strength dependence of the equilibrium association constant [31]. A model for the CCP(III)/cyt c(III) complex which was generated, by computer graphics modelling, by optimizing hydrogen bonding interactions between complementary charged groups [8] is given in Figure 3.1. Notice that the CCP substrate access channel, which connects the edge of pyrrole IV to the molecular surface of CCP, is not blocked by complex formation. However, the exposed heme edge of cyt c appears to be surrounded by protein when it is bound to CCP. Several kinetic experiments support this model. Studies have shown that the rate of reaction of CCP with hydrogen peroxide [32] and fluoride [33] is unaffected by the presence of cyt c. Holth and Erman [33] have shown that complex formation decreases the rate of cyanide binding to horse cyt c by about 90%. Mochan and Nicholls [32] have observed that the reduction of cyt c(III) by ascorbate is hindered by $\approx$ 90% upon complex formation with CCP. Hazzard et al. [34] have reported that the rates of reduction of yeast iso-2 and horse cyt c(III), by flavin semiquinones (which are radical anions) produced by laser flash photolysis, are decreased by 91 and 74%, respectively, in their CCP complexes. Clearly, the accessibility of the hemes of cyts c is reduced in the presence of CCP. However, in these experiments, the small reagents are all negatively charged so it is difficult to differentiate between electrostatic repulsion and steric interactions, due to
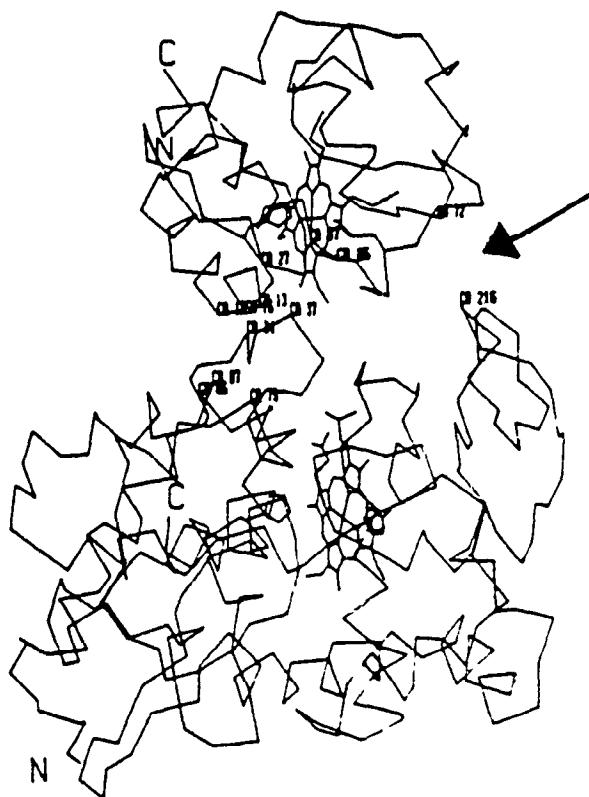
Figure 3.1. Hypothetical CCP/cyt c complex. Yeast CCP is at the bottom and tuna

cyt c at the top. Note that the access channel of CCP (at arrow)

remains open, and that the exposed heme of cyt c is blocked by CCP.

the presence of the negatively charged peroxidase, as possible causes for the decrease in heme accessibility of cyt c.

To further probe the environment near the heme edge of cyt c, we have investigated the effect of complex formation on the rate of NO binding by cyt c. As discussed in Chapter 1, NO can readily penetrate into the hydrophobic heme crevice and bind to the Fe(III) atom of cyt c. Because it is a neutral small molecule, its binding to cyt c will not be affected by electrostatic interactions. Therefore, the accessibility of the heme of cyt c in the CCP/cyt c complex can be probed by measuring the on-rates between cyt c(III) and NO in the absence and presence of CCP:

$$\text{cyt c(III)} + \text{NO} \xrightleftharpoons{k_{on}} \text{cyt c(III)-NO} \tag{3.1}$$

$$\text{CCP(III)/cyt c(III)} + \text{NO} \xrightleftharpoons{k'_{on}} \text{CCP(III)/cyt c(III)-NO} \tag{3.2}$$
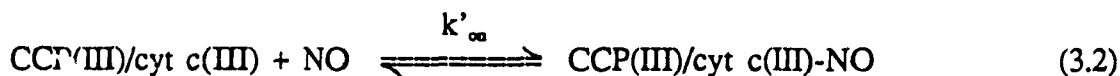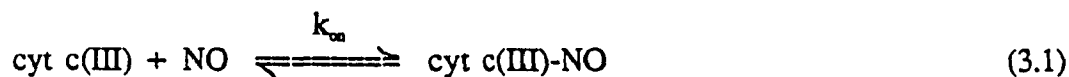
In rx 3.2, CCP(III) is actually CCP(III)-NO, however, since NO binding to CCP(III) is rapid (6.6 X $10^5 M^{-1}$ s^{-1}, Table 1.VI) it will not interfere with the slow reaction of NO binding to cyt c. Reactions 3.1 and 3.2 are compared here for both horse and yeast cyts c. Data on reaction 3.1 for horse cyt c were already presented in Chapter 1.

3.2 EXPERIMENTAL

MATERIALS- Yeast CCP was isolated by the published procedure [12], and type VI horse heart and type VIII-A Saccharomyces cerevisiae cyt c were obtained from Sigma. Nitric oxide (CP grade) was obtained from Union Carbide and was passed through KOH pellets before use to remove any higher oxides of nitrogen. The concentrations of cyt c and NO were varied from 2.5 to 4.7 μM, and 95 to 1000 μM, respectively. CCP was present in a slight excess over cyt c.

METHODS- Kinetic measurements were carried out in 10 mM sodium r μphate, at pH 7.0, and 23 °C using the procedures given in the methods section of Chapter 1. A series of on-rates for the binding of NO by cyt c(III) was measured, in the presence and absence of CCP(III), at various [NO]. NO binding by cyt c(III) was monitored by following the absorbance growth at 418 nm [$\Delta\varepsilon$ (cyt c-NO - cyt c) = 39 mM^{-1} cm^{-1} (Figure 1.7)] in the 2-mm cuvette of a modified HI-TECH SFA-11 Fast Kinetics Accessory stopped-flow unit using the fast response time (0.1 s) of the HP Model 8451A spectrophotometer.

3.3 DATA ANALYSES

All kinetic data were analyzed by the Simplex nonlinear regression method [17] (see Data Analysis in Chapter 1).

3.4 RESULTS

The rates of NO binding by horse and yeast cyts c(III) were investigated in the presence and absence of CCP(III), and the results are discussed separately for each cyt c.

3.4.1. Horse Cyt c-NO Formation:

Only a single reaction was observed upon mixing horse cyt c(III) and NO, in the presence and absence of CCP, in the stopped-flow, and Figure 3.2 shows typical reaction time courses. The Simplex nonlinear regression method [17] yielded the first-order fits of the observed absorbance growths as shown in Figure 3.2, and the observed rate constants (k_{obs}) are listed in Table 3.I.

Plots of k_{obs} versus NO concentration gave straight lines with slopes equal to the bimolecular rate constant (k_{on}) for the binding of NO by cyt c(III). These plots are shown in Figure 3.3 and the values for k_{on} in the presence and absence of CCP are 305 ± 43 M^{-1} s^{-1} and 417 ± 60 M^{-1} s^{-1}, respectively. Therefore, the rates of NO binding by cyt c are reduced by $\approx 27\%$ when cyt c is complexed with CCP. If the point at 1000 μM NO in Figure 3.3, in the presence of CCP, is removed then the rates of NO binding by cyt c(III) would have decreased by 45%.
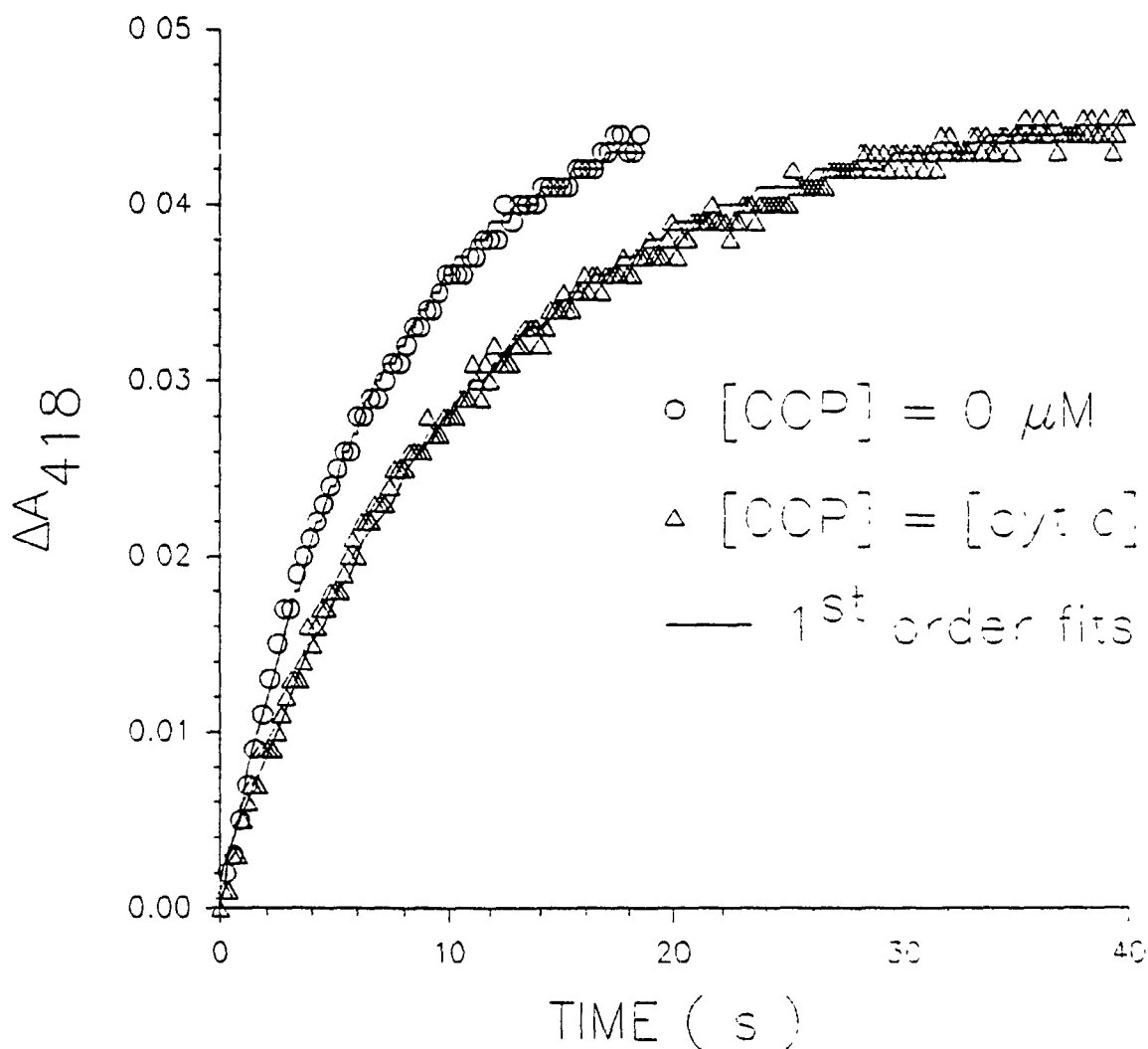
Figure 3.2. Reaction time courses for the binding of NO by horse cyt c(III) in the presence and absence of CCP(III) at 418 nm in 10 mM sodium phosphate buffer, pH 7.0, 23 °C. [NO]= 333 μM and [cyt c]= 4.13 μM. The solid line is the calculated first-order fit using the Simplex nonlinear regression method (see Data Analyses).

Table 3.I. Observed Rate Constants (k_{obs}) for The Binding of Nitric Oxide by Horse Cyt c in The Presence and Absence of CCP(III) in 10 mM Phosphate Buffer, pH 7.0, 23 °C

[NO] (μM)	k_{obs} (s^{-1})	
	Free Cyt c	CCP-Complexed Cyt c
95	0.07 ± .01	0.045 ± .006
185	0.11 ± .02	0.073 ± .011
333	0.15 ± .02	0.089 ± .013
666	0.31 ± .04	0.18 ± .02
1000	------	0.33 ± .05

Figure 3.3. Plots of the observed rate constants as a function of [NO] for the binding of NO by horse cyt c(III) in the presence and absence of CCP in 10 mM sodium phosphate, pH 7.0, 23 °C.

The observed rate constants (k_{obs}), in the presence of increasing [CCP(III)] are listed in Table 3.II. A CCP/cyt c ratio of 1:1 reduces the k_{obs} for NO binding to cyt c by $\approx$ 30% as shown in Figure 3.4. This indicates that most of the cyt c was complexed with CCP at the concentrations of CCP used in the experiments described above.

Table 3.II. Observed Rates Constants for the Binding of 333 μM

NO by 3.0 μM Cyt c(III), in The Presence of Increasing

[CCP(III)], in 10 mM Phosphate Buffer, pH 7.0, 23 °C

[CCP] (μM)	k_{obs} (s^{-1})
0	0.15 ± 0.01
1.5	0.13 ± 0.01
3.0	0.101 ± 0.005
4.5	0.100 ± 0.005
9.0	0.099 ± 0.005
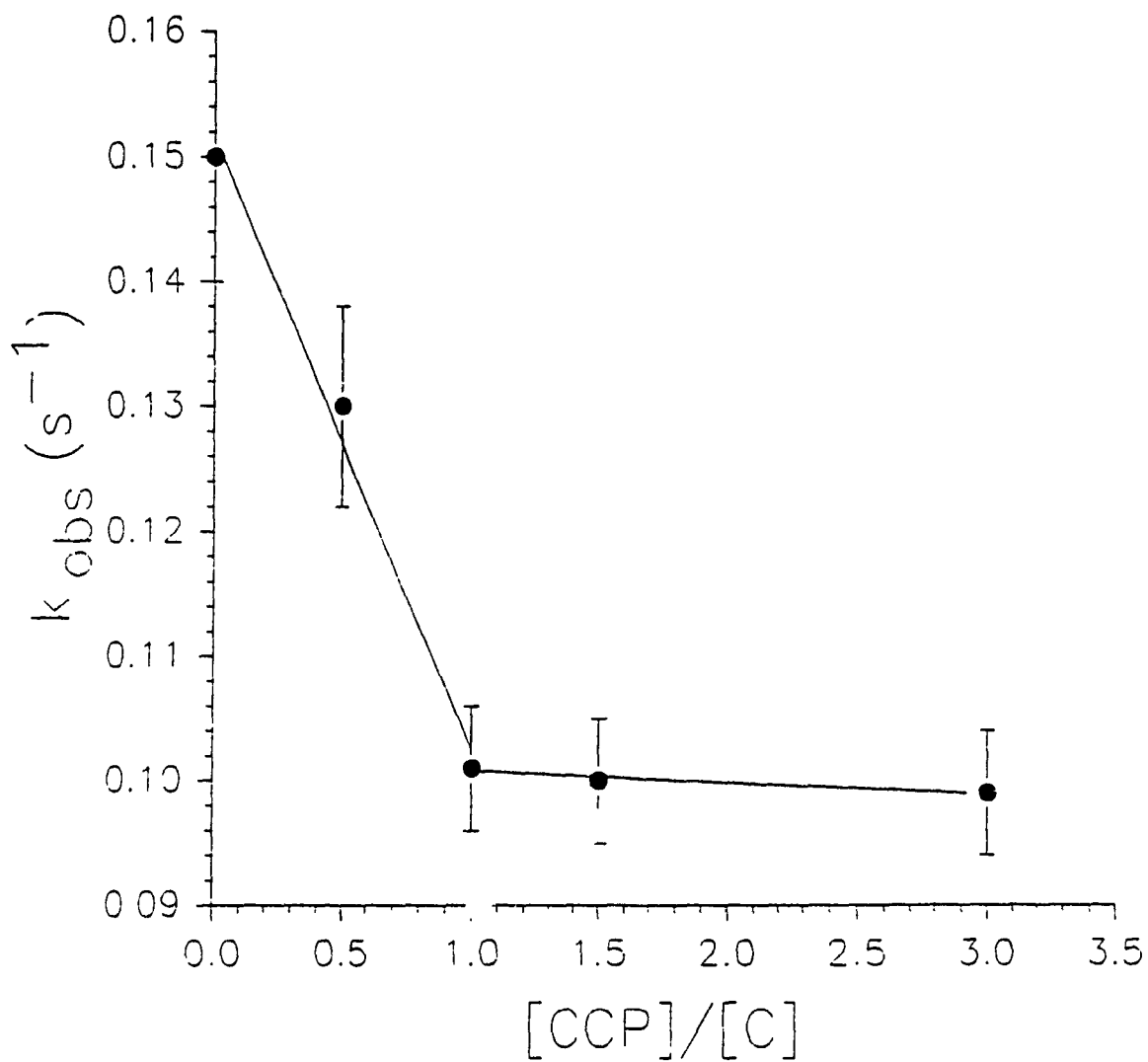
Figure 3.4. The observed pseudo first-order rate constants for the binding of

333 μM NO by 3.0 μM horse cyt c(III) versus the ratio of

[CCP]/[cyt c]. The reaction was carried out in 10 mM sodium

phosphate buffer, pH 7.0, 23 °C.

3.4.2. Yeast Cyt c-NO Formation:

As in the case of horse cyt c, only a single reaction was observed upon mixing yeast cyt c and NO, in the presence and absence of CCP, in the stopped-flow. Furthermore, a simple first order equation was fitted to all the reaction time courses using the Simplex nonlinear regression method, and the observed rate constants (k_{obs}) are listed in Table 3.III.

Plots of k_{obs} versus NO concentration gave straight lines with slopes equal to the bimolecular rate constant (k_{on}) for the binding of NO by cyt c(III) These plots are shown in Figure 3.5 and the values for k_{on} in the presence and absence of CCP are 96 ± 13 M^{-1} s^{-1} and 365 ± 51 M^{-1} s^{-1}, respectively. Therefore, the rates of NO binding by yeast cyt c are reduced by ≈ 74% when cyt c is complexed with CCP.

Under the ionic strength conditions employed in this experiment, yeast cyt c should also bind tightly to CCP. Kang et al. [35] have shown that the K_D for complex formation between yeast and horse cyts c with CCP are very similar and equal to ≈ 2 X 10^{-7} M in 0.01 M Tris/chloride buffer. Therefore, it was assumed that most of the yeast cyt c would be complexed to CCP at a [CCP]/[cyt c] ratio of 1:1.

Table 3.III. Observed Rate Constants (k_{obs}) for The Binding of NO by

Yeast Cyt c in The Presence and Absence of CCP(III) in 10

mM Phosphate Buffer pH 7.0, 23 °C

[NO] (μM)	k_{obs} (s^{-1})	
	Free Cyt c	CCP-Complexed Cyt c
95	0.045 ± .006	------
185	0.068 ± .010	------
333	0.091 ± .014	0.020 ± .003
666	0.233 ± .035	0.044 ± .007
1000	0.367 ± .055	0.084 ± .013
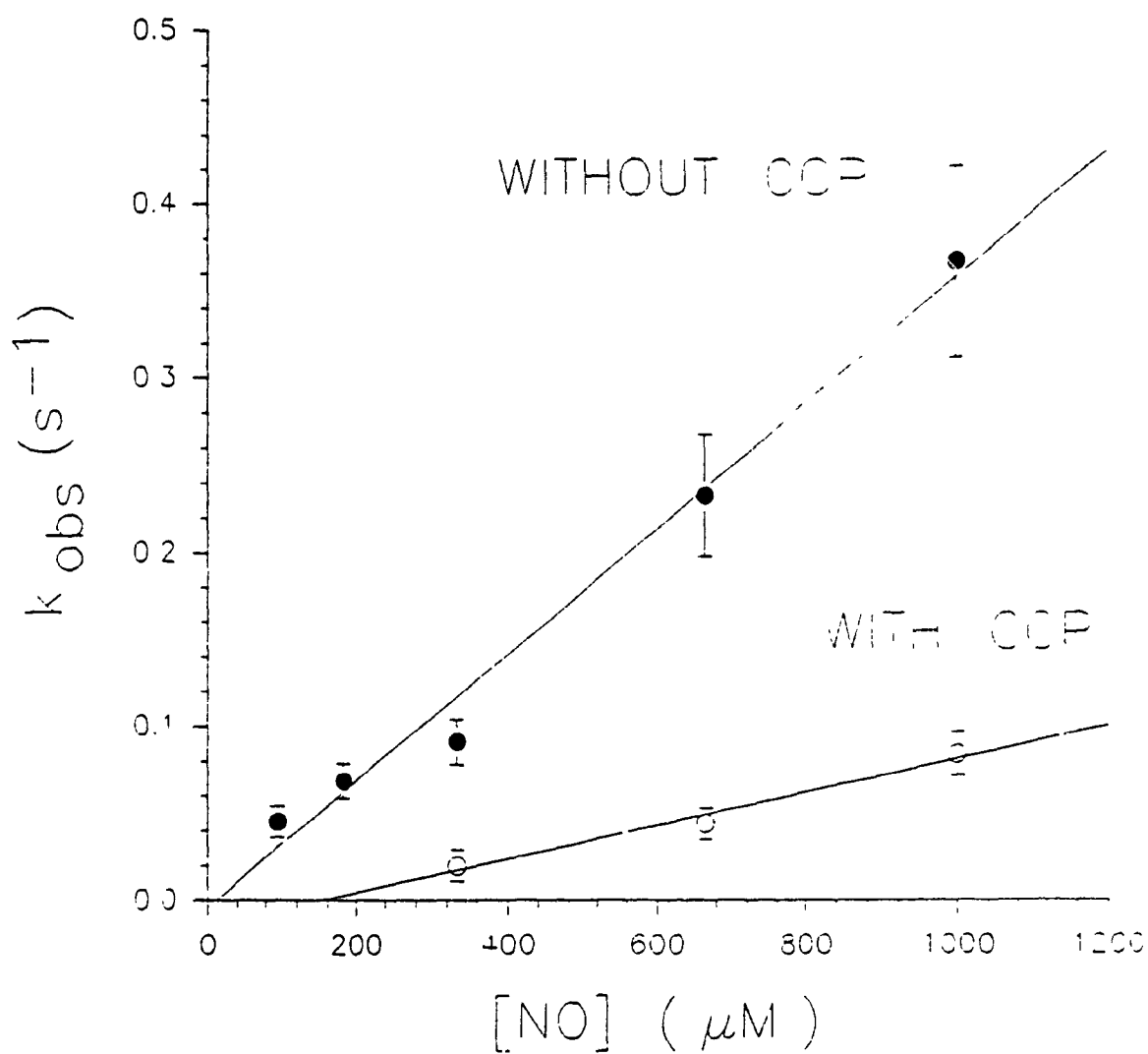
Figure 3.5. Plots of the observed rate constants versus [NO] for the binding
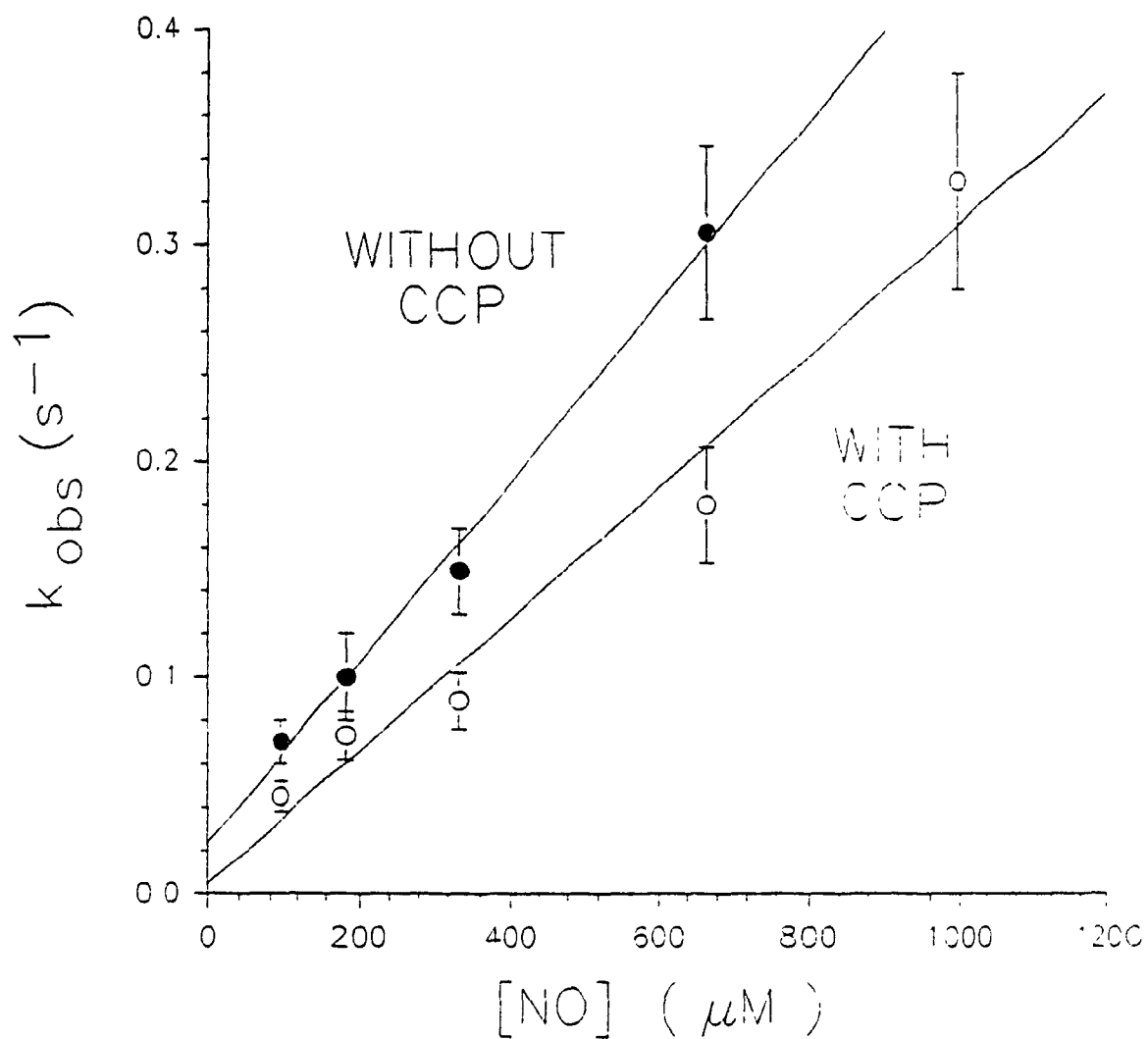
of NO by yeast cyt c(III) in the presence and absence of CCP

in 10 mM sodium phosphate, pH 7.0, 23 °C.

3.5 DISCUSSION

The bimolecular rate constants for the binding of NO by free and complexed cyts c are listed in Table 3.IV. The on-rates for the binding of NO by free horse cyt c is $\approx$ 1.1 times faster than that by yeast cyt c. A comparison of the X-ray crystal structures of the two proteins indicates that a portion of the heme edge of horse cyt c is exposed to solvent [36], but the heme group of yeast cyt c appears to be completely surrounded by protein matrix [37]. Therefore, NO may react faster with horse cyt c since it may not have to diffuse as far through the protein matrix.

The on-rates for the binding of NO by horse and yeast cyts c decrease by 27-45% and 74%, respectively, in the presence of CCP. The reduction in the on-rates between NO, a neutral molecule, and cyts c(III) is probably due to the fact that CCP physically blocks the access pathway to the hemes of cyts c in the CCP/cyt c complexes. However, in a similar study, Holth and Erman [33, 38] report that complex formation between horse cyt c(III) and CCP decreases the on-rate for the binding of CN$^-$ by horse cyt c(III) by 90%. Other negatively small charged species [34, 32], have also been used to probe the heme accessibility of cyts c in the CCP/cyt c complexes, and they show that complex formation reduces accessibility to the heme of cyt c by 74% for horse cyt c, and 90% for yeast cyt c. Therefore, in the latter experiments, electrostatic repulsion between the negatively charged CCP and the reagents probably contributed to the reduction of heme accessibility of cyt c. Furthermore, notice that the accessibility to the heme of horse

Table 3.IV. Bimolecular Rate Constants for the Binding of NO by Horse

and Yeast Cyts c in the Presence and Absence of CCP

cyt c	k_{on} (M^{-1} s^{-1})		Decrease in k_{on} in the presence of CCP
	Free cyt c	Complexed cyt c	
Horse	417 ± 60	305 ± 43	27%
Yeast	365 ± 51	96 ± 13	74%

cyt c is more affected by the presence of CCP when CN⁻ is used as a probe. This is probably due to the fact that CN⁻ is more repelled by CCP than the other reagents, since CN⁻ is a small molecule and its negative charge is not delocalized.

CCP may also stabilize the native conformations of cyt c. Osheroff et al. [39] have shown that binding of carbonate and phosphate anions to the surface of horse cyt c increases the stability of the closed heme crevice structure. Carbonate and phosphate anions bind with high affinity to sites near the heme crevice and increases the pK_a of the closed heme crevice, derived from the measurements of the 695 nm absorption bands. Since the pK_a of the 695 nm absorption bands is observed only in the presence of the Fe(III)-Met-80 bond, the pK_a values are an indication of the ease with which the heme crevice can be opened. CCP, which is an anion, may also stabilize the closed heme structures of yeast and horse cyts c, and thus reduce the on-rates for the binding of NO. However, the effect of CCP complexation on the stability of the Fe(III)-Met bond of cyt c has not been investigated. So the importance of anionic binding to the surface of cyt c in controlling heme accessibility of cyts c is not known. In order to probe the stability of the heme crevice of cyt c, the concentration of NO would have to be increased to the point where heme crevice opening becomes the rate limiting step for NO binding to cyt c.

Finally, a comparison of the NO on-rates shows that the complexes formed between the cyts c and CCP are not equivalent. For example, a tighter fit between yeast cyt c and CCP should reduce the heme accessibility of yeast cyt c more than horse cyt c. Thus, the NO data are consistent with the idea that yeast cyt c and CCP form a tighter fit because they are biological electron transfer partners in yeast.

CONTRIBUTIONS TO KNOWLEDGE

1. Cyt c and its peroxidase, which have different heme cavities, form NO-adducts with approximately the same stability.

2. Cyt c, which has 2 stable axial ligands, has slow on and off rates for the binding of NO to the Fe(III) atom. The on and off rates for NO binding by CCP(III) are similar to that of other heme proteins.

3. NO coordination to CCP increases the Fe(III)/(II) reduction potential by 250-300 mV. This is consistent with the observed increased stability of Fe(II)-NO.

4. Nitric oxide coordination to the iron atom of CCP(II) slows down the rate of intracomplex electron transfer from CCP(II) to cyt c(III) at least 40 fold. This may be due to the drop in driving force, and/or perturbation of the peroxidase on binding NO.

5. Complex formation between CCP(III) and cyt c(III) reduces the heme accessibility of horse and yeast cyts c by 30 ± 10% and 74%, respectively.

SUGGESTIONS FOR FURTHER STUDIES

Chapter 1. Measure on-rates for the binding of NO by CCP(III) at various

[NO], and verify that the ratio of the kinetic rate constants (k_{off}/k_{obs})

is similar to the equilibrium binding constant. Also, direct

measurements of NO off-rates for both proteins would support

the kinetic data.

Chapter 2. Prepare CCP(II) in a glove box, and remove excess reductant by

colunm chromatography. This would eliminate unwanted cyt c(III)

reduction and CCP(II)-NO decay. If a reaction is still observed, then one

should measure $\Delta E^{\ddagger}$ to determine whether or not the reaction is rate

limited by NO dissociation from the Fe(II) or electron transfer from

CCP(II)-NO. A large $\Delta E^{\ddagger}$ would be consistent with bond cleavage while

a small $\Delta E^{\ddagger}$ would indicate that electron transfer is the limiting step of

the reaction.

Chapter 3. Measure on-rates for the binding of NO to cyt c(III) at various ionic

strengths. This would allow one to probe the heme accessibility of cyt

c as a function of ionic strength. This is important since changes in the

electrostatically stabilizea CCP/cyt c complex may be linked to changes

in the rates of intracomplex electron transfer.

REFERENCES

1. Coletta, M., Ascoli, F., Brunori, M., & Traylor, T. G. (1986) *J. Biol. Chem.* **261**, 9811.

2. Yonetani, T., Yamamoto, H., Erman, J. E., Leigh, J. S., & Reed, G. H. (1972) *J. Biol. Chem.* **247**, 2447.

3. Butt, W D., & Keilin, D. (1962) *Proc. R. Soc. London* **156**, 429.

4. Bechtold, R., Gardineer, M. B., Kazmi, A., van Hemelryck, B., & Isied, S. S. (1986) *J. Phys. Chem.* **90**, 3800.

5. Finzel, B. C., Poulos, T. L., & Kraut, J. (1984) *J. Biol. Chem.* **259**, 13027.

6. Edwards, S. L., Kraut, J., & Poulos, T. L. (1988) *Biochemistry* **27**, 8074.

7. Dickerson, R. E., Takano, T., Eisenberg, D., Kallai, O.B., Samson, L., Cooper, A., & Margoliash, E. (1971) *J. Biol. Chem.* **246**, 1511.

8. Poulos, T. L., & Kraut, J. (1980) *J. Biol. Chem.* **255**, 10322.

9. Sharma, S., V., Traylor, T. G., & Gardiner, R. (1987) *Biochemistry* **26**, 3837.

10. Mims, M., P., Porras, A. G., Olson, J. S., Noble, W. R., & Peterson, J. A. (1983) *J. Biol. Chem.* **258**, 14219.

11. Anderson, S. R., & Antonini, E. (1968) *J. Biol. Chem.* **243**, 2918.

12. English, A. M., Laberge, M., & Walsh, M. (1986) *Inorg. Chim. Acta.* **123**, 113.

13. Yonetani, T., & Anni, H. (1987) *J. Biol. Chem.* **262**, 9547.

14. Margoliash, E., & Frohwirt, N. (1959) *Biochem. J.* **71**, 570.

15. Shaw, A. W., & Vosper, A. J. (1977) *J. Chem. Soc.*, *Faraday Trans.* 1, 1239.

16. Harris, D. C., W. H. Quantitative Chemical Analysis, Freeman and Company, New York, 1982, p. 517.

17. Caceci, M. S., & Cacheris, W. P. (1984) *Byte* 9, N° 5, 340.

18. Hiromi, K. Kinetics of Fast Enzyme Reactions, John Wiley & Sons, Tokyo, 1979, p 219.

19. Smulevich, G., Mauro, J. M., Fishel, L. A., English, A. M., Kraut, J., & Spiro, T. G. (1988) *J. Am. Chem. Soc.* 27, 5477.

20. Poulos, T. L., Freer, S. T., Alden, R. A., Xuong, N., Edwards, S. L., Hamlin, R. C., & Kraut, J. (1978) *J. Biol. Chem.* **253**, 3730.

20a. Creutz, C., & Sutin, N. (1974) *J. Biol. Chem.* **249**, 6788.

21. Ala, P., & Cheung, E. Unpublished observations.

22. English, A. M., Cheung, T. C., & Kornblatt, J. A. (1985) *Rev. Port. Quim.* 27, 237.

23. Erman, J. E. (1974) *Biochemistry* 13, 39.

24. Erman, J. E. (1974) *Biochemistry* 13, 34.

25. Sharma, V. S., Isaacson, R. A., John, M. E., Waterman, M. R., & Chevion, M. (1983) *Biochemistry* 22, 3897.

25a. Mauro, J. M., Fishel, L. A., Hazzard, J. T., Meyer, T. E., Tollin, G., Cusanovich, M. A., & Kraut, J. (1988) *Biochemistry* 27, 6243.

26. Ward, B., & Chang, C. K. (1982) *Photochem. Photobiol.* **35**, 757.

27. Yocom, K. M. The Synthesis and Characterization of Inorganic Redox Reagents, Ph.D. thesis, California Institute of Technology, Pasadena, California, 1982.

28. Creutz, C., & Sutin, N. (1973) *Proc. Nat. Acad. Sci. USA* **70**, 1701.

29. Yee, E. L., Cave, R. J., Guyer, K. L., Tyma, P. D., Weaver, M. J. (1979) *J. Am. Chem. Soc.* **1**, 1131.

30. Conroy, C. W., Tyma, P., Daum, P. H., & Erman, J. E. (1978) *Biochim. Biophys. Acta* **537**, 62.

31. Ermam,J. E., & Vitello, L. B. (1980) *J. Biol. Chem.* **255**, 6224.

32. Nicholls, P., & Mochan,E. (1971) *Biochem. J.* **121**, 55.

33. Holth, L. R., & Erman, J. E. (1984) *Biochim. Biophys. Acta* **788**, 151.

34. Hazzard, J. T., Poulos, T. L., & Tollin, G. (1987) *Biochemistry* **26**, 2836.

35. Kang, C.H., Ferguson-Miller, S., & Margoliash, E. (1977) *J. Biol. Chem.* **252**, 919.

36. Dickerson, R. E., Takano, T., Eisenberg, D., Kallai, O., B., Samson, L., Cooper, A., & Margoliash, E. (1971) *J. Biol. Chem.* **246**, 1511.

37. Louie, G., V., Hutcheon W., L., B., & Brayer, G. D. (1988) *I. Mol. Biol.* **199**, 295.

38. Personal communication with J. E. Erman

39. Osheroff, N., Brautigan, D. L., & Margoliash, E. (1980) *Proc. Natl. Sci. USA* **77**, 4439.

APPENDIX A

SCATCHARD PLOT DATA
FOR CCP(III)-NO FORMATION

TABLE I

SCATCHARD PLOT #1
[CCP] = 2.51 uM

$$K = 52.1 uM$$

At (424 nm)	*Ac (424 nm)	[NO] (uL)	Ac-Ao	[NO] (uM)	(Ac-Ao)/[NO] (uM)
0.2019	0.2038	40.0000	0.0536	18.6480	0.0029
0.2137	0.2167	60.0000	0.0665	27.8422	0.0024
0.2334	0.2389	100.0000	0.0887	45.9770	0.0019
0.2504	0.2592	150.0000	0.1090	68.1818	0.0016
0.2596	0.2718	200.0000	0.1216	89.8876	0.0014
0.2703	0.2894	300.0000	0.1392	131.8681	0.0011
0.2720	0.2976	400.0000	0.1474	172.0430	0.0009
0.2725	0.3046	500.0000	0.1544	210.5263	0.0007
0.2730	0.3115	600.0000	0.1613	247.4227	0.0007
0.2715	0.3162	700.0000	0.1660	282.8283	0.0006
0.2688	0.3194	800.0000	0.1692	316.8317	0.0005
0.2640	0.3199	900.0000	0.1697	349.5146	0.0005

*Ac is the observed absorbance at 424 nm which has been corrected for dilution after each addition of NO-saturated buffer

TABLE II

SCATCHARD PLOT #2
[CCP] = 3.28 uM

$K = 40.7 uM$

At (424 nm)	*Ac (424 nm)	[NO] (uL)	Ac-Ao	[NO] (uM)	(Ac-Ao)/ [NO] (uM)
0.2550	0.2574	40.0000	0.0770	18.8679	0.0041
0.2772	0.2812	60.0000	0.1008	28.1690	0.0036
0.2880	0.2935	80.0000	0.1131	37.3832	0.0030
0.2965	0.3036	100.0000	0.1232	46.5116	0.0026
0.3138	0.3250	150.0000	0.1446	68.9655	0.0021
0.3256	0.3411	200.0000	0.1607	90.9091	0.0018
0.3350	0.3510	250.0000	0.1706	112.3596	0.0015
0.3424	0.3628	300.0000	0.1824	133.3333	0.0014
0.3443	0.3689	400.0000	0.1885	173.9130	0.0011
0.3466	0.3796	500.0000	0.1992	212.7660	0.0009
0.3461	0.3873	600.0000	0.2069	250.0000	0.0008
0.3433	0.3923	700.0000	0.2119	285.7143	0.0007
0.3407	0.3975	800.0000	0.2171	320.0000	0.0007

*Ac is the observed absorbance at 424 nm which has been corrected for dilution after each addition of NO-saturated buffer

TABLE III

SCATCHARD PLOT #3
[CCP] = 3.64 uM

$$K = 43.6 uM$$

At (424 nm)	*Ac (424 nm)	[NO] (uL)	Ac-Ao	[NO] (uM)	(Ac-Ao)/ [NO] (uM)
0.2822	0.2849	40.0000	0.0799	19.8020	0.0040
0.2984	0.3027	60.0000	0.0977	29.5567	0.0033
0.3154	0.3214	80.0000	0.1164	39.2157	0.0030
0.3258	0.3336	100.0000	0.1286	48.7805	0.0026
0.3497	0.3622	150.0000	0.1572	72.2892	0.0022
0.3592	0.3763	200.0000	0.1713	95.2381	0.0018
0.3695	0.3871	250.0000	0.1821	117.6471	0.0015
0.3729	0.3951	300.0000	0.1901	139.5349	0.0014
0.3777	0.4047	400.0000	0.1997	181.8182	0.0011
0.3741	0.4097	500.0000	0.2047	222.2222	0.0009
0.3740	0.4185	600.0000	0.2135	260.8696	0.0008

*Ac is the observed absorbance at 424 nm which has been corrected for dilution after each addition of NO-saturated buffer

TABLE IV

SCATCHARD PLOT #4
[CCP] = 4.39 uM

K = 44.2uM

At (424 nm)	*Ac (424 nm)	[NO] (uL)	Ac-Ao	[NO] (uM)	(Ac-Ao)/[NO] (uM)
0.3491	0.3524	40.0000	0.0929	18.8679	0.0049
0.3728	0.3781	60.0000	0.1186	28.1690	0.0042
0.3920	0.3995	80.0000	0.1400	37.3832	0.0037
0.4089	0.4186	100.0000	0.1591	46.5116	0.0034
0.4330	0.4485	150.0000	0.1890	68.9655	0.0027
0.4487	0.4701	200.0000	0.2106	90.9091	0.0023
0.4622	0.4952	300.0000	0.2357	133.3333	0.0018
0.4643	0.4975	400.0000	0.2380	173.9130	0.0014
0.4601	0.5039	500.0000	0.2444	212.7660	0.0011
0.4522	0.5060	600.0000	0.2465	250.0000	0.0010

*Ac is the observed absorbance at 424 nm
which has been corrected for dilution
after each addition of NO-saturated buffer

TABLE V

SCATCHARD PLOT #5
[CCP] = 4.41 uM

K = 44.5uM

At (424 nm)	*Ac (424 nm)	[NO] (uL)	Ac-Ao	[NO] (uM)	(Ac-Ao)/ [NO] (uM)
0.3389	0.3421	40.0000	0.0976	18.4332	0.0053
0.3657	0.3708	60.0000	0.1263	27.5229	0.0046
0.3826	0.3897	80.0000	0.1452	36.5297	0.0040
0.3948	0.4040	100.0000	0.1595	45.4545	0.0035
0.4232	0.4380	150.0000	0.1935	67.4157	0.0029
0.4381	0.4585	200.0000	0.2140	88.8889	0.0024
0.4486	0.4747	250.0000	0.2302	109.8901	0.0021
0.4530	0.4846	300.0000	0.2401	130.4348	0.0018
0.4587	0.5014	400.0000	0.2569	170.2128	0.0015
0.4579	0.5111	500.0000	0.2666	208.3333	0.0013
0.4566	0.5203	600.0000	0.2758	244.8980	0.0011
0.4520	0.5256	700.0000	0.2811	280.0000	0.0010
0.4466	0.5297	800.0000	0.2852	313.7255	0.0009
0.4438	0.5367	900.0000	0.2922	346.1538	0.0008

*Ac is the observed absorbance at 424 nm
which has been corrected for dilution
after each addition of NO-saturated buffer

TABLE VI

SCATCHARD PLOT #6
[CCP] = 4.74 uM

K = 45.2uM

At (424 nm)	*Ac (424 nm)	[NO] (uL)	Ac-Ao	[NO] (uM)	(Ac-Ao)/ [NO] (uM)
0.3329	0.3345	20.0000	0.0625	9.4787	0.0066
0.3481	0.3506	30.0000	0.0786	14.1844	0.0055
0.3643	0.3678	40.0000	0.0958	18.8679	0.0051
0.3927	0.3983	60.0000	0.1263	28.1690	0.0045
0.4031	0.4098	70.0000	0.1378	32.7869	0.0042
0.4111	0.4189	80.0000	0.1469	37.3832	0.0039
0.4176	0.4256	90.0000	0.1536	41.9580	0.0037
0.4234	0.4325	100.0000	0.1605	46.5116	0.0035
0.4541	0.4649	150.0000	0.1929	68.9655	0.0028
0.4710	0.4878	200.0000	0.2158	90.9091	0.0024
0.4828	0.5058	250.0000	0.2338	112.3596	0.0021
0.4872	0.5162	300.0000	0.2442	133.3333	0.0018
0.4917	0.5268	400.0000	0.2548	173.9130	0.0015
0.4930	0.5400	500.0000	0.2680	212.7660	0.0013
0.4907	0.5491	600.0000	0.2771	250.0000	0.0011
0.4862	0.5557	700.0000	0.2837	285.7143	0.0010
0.4819	0.5622	800.0000	0.2902	320.0000	0.0009
0.4773	0.5682	900.0000	0.2962	352.9412	0.0008

*Ac is the observed absorbance at 424 nm
which has been corrected for dilution
after each addition of NO-saturated buffer

TABLE VII

SCATCHARD PLOT #7
[CCP] = 4.89 uM

K = 35.1 uM

At (424 nm)	*Ac (424 nm)	[NO] (uL)	Ac-Ao	[NO] (uM)	(Ac-Ao)/[NO] (uM)
0.4018	0.4075	60.0000	0.1401	28.1690	0.0050
0.4253	0.4334	80.0000	0.1660	37.3832	0.0044
0.4389	0.4494	100.0000	0.1820	46.5116	0.0039
0.4644	0.4810	150.0000	0.2136	68.9655	0.0031
0.4783	0.5011	200.0000	0.2337	90.9091	0.0026
0.4887	0.5119	250.0000	0.2445	112.3596	0.0022
0.4975	0.5271	300.0000	0.2597	133.3333	0.0019
0.5079	0.5442	400.0000	0.2768	173.9130	0.0016
0.5033	0.5512	500.0000	0.2838	212.7660	0.0013
0.4966	0.5557	600.0000	0.2883	250.0000	0.0012
0.4910	0.5611	700.0000	0.2937	285.7143	0.0010
0.4855	0.5664	800.0000	0.2990	320.0000	0.0009

*Ac is the observed absorbance at 424 nm
which has been corredted for dilution
after each addition of NO-saturated buffer

APPENDIX B

SCATCHARD PLOT DATA
FOR CYT C(III)-NO FORMATION

TABLE I

SCATCHARD PLOT #1
[Cyt c] = 3.17 uM

K = 34.5uM

At (418 nm)	*Ac (418 nm)	[NO] (uL)	Ac-Ao	[NO] (uM)	(Ac-Ao)/[NO] (uM)
0.3082	0.3111	40.0000	0.0723	18.8679	0.0038
0.3270	0.3317	60.0000	0.0929	28.1690	0.0033
0.3390	0.3455	80.0000	0.1067	37.3832	0.0029
0.3500	0.3583	100.0000	0.1195	46.5116	0.0026
0.3560	0.3662	120.0000	0.1274	55.5556	0.0023
0.3700	0.3850	170.0000	0.1462	77.8032	0.0019
0.3744	0.3896	220.0000	0.1508	99.5475	0.0015
0.3815	0.4015	320.0000	0.1627	141.5929	0.0011
0.3820	0.4111	400.0000	0.1723	173.9130	0.0010
0.3790	0.4151	500.0000	0.1763	212.7660	0.0008

*Ac is the observed absorbance at 418 nm
which has been corrected for dilution
after each addition of NO-saturated buffer

TABLE II

SCATCHARD PLOT #2
[Cyt c] = 4.75 uM

K = 39.7uM

At (418 nm)	xAc (418 nm)	[NO] (uL)	Ac-Ao	[NO] (uM)	(Ac-Ao)/ [NO] (uM)
0.4491	0.4534	40.0000	0.1023	18.8679	0.0054
0.4782	0.4850	60.0000	0.1339	28.1690	0.0048
0.4981	0.5076	80.0000	0.1565	37.3832	0.0042
0.5139	0.5261	100.0000	0.1750	46.5116	0.0038
0.5231	0.5380	120.0000	0.1869	55.5556	0.0034
0.5354	0.5532	140.0000	0.2021	64.5161	0.0031
0.5392	0.5572	160.0000	0.2061	73.3945	0.0028
0.5526	0.5737	200.0000	0.2226	90.9091	0.0024
0.5635	0.5903	250.0000	0.2392	112.3596	0.0021
0.5663	0.6000	300.0000	0.2489	133.3333	0.0019
0.5695	0.6102	400.0000	0.2591	173.9130	0.0015

xAc is the observed absorbance at 418 nm
which has been corrected for dilution
after each addition of NO-saturated buffer

TABLE III

SCATCHARD PLOT #3
[Cyt c] = 5.90 uM

K = 34.6 uM

At (418 nm)	*Ac (418 nm)	[NO] (uL)	Ac-Ao	[NO] (uM)	(Ac-Ao)/ [NO] (uM)
0.5937	0.6022	60.0000	0.1650	27.5229	0.0060
0.6191	0.6309	80.0000	0.1937	36.5297	0.0053
0.6348	0.6499	100.0000	0.2127	45.4545	0.0047
0.6427	0.6611	120.0000	0.2239	54.2986	0.0041
0.6582	0.6801	140.0000	0.2429	63.0631	0.0039
0.6761	0.6986	180.0000	0.2614	80.3571	0.0033
0.6904	0.7200	240.0000	0.2828	105.7269	0.0027
0.6944	0.7341	300.0000	0.2969	130.4348	0.0023
0.6944	0.7440	400.0000	0.3068	170.2128	0.0018

*Ac is the observed absorbance at 418 nm
which has been corrected for dilution
after each addition of NO-saturated buffer